SUPPORTING INFORMATION

Diarylethene moiety as an enthalpy-entropy switch: photoisomerizable stapled peptides for modulating p53/MDM2 interaction

Alexander V. Strizhak, Oleg Babii, Sergii Afonin, Iuliia Bakanovich, Teodors Pantelejevs, Wenshu Xu, Elaine Fowler, Rohan Eapen, Krishna Sharma, Maxim O. Platonov, Vasyl V. Hurmach, Laura Itzhaki, Marko Hyvönen, Anne S. Ulrich*, David R. Spring* and Igor V. Komarov*

*Correspondence: Anne.Ulrich@kit.edu, Spring@ch.cam.ac.uk, Igor.Komarov@lumobiotics.com

TABLE OF CONTENT

General information

Solvents and reagents
All chemicals, reagents for peptide synthesis, and solvents were purchased from Merck (Sigma-Aldrich), Fischer, ABCR, Iris Biotech, and Biosolve. Tetrahydrofuran (THF) and N,N-diisopropylethylamine (DIPEA) were freshly distilled under an argon atmosphere from sodium with benzophenone as an indicator.

Chromatography
Column chromatography was carried out using Kieselgel 60 silica (230-400 mesh) under a pressure of nitrogen gas. Thin-layer chromatography was carried out on glass plates Merck Kieselgel 60 F254 and visualized by ultraviolet irradiation (at 254 and 365 nm).

Nuclear magnetic resonance (NMR) spectroscopy
Analytical NMR spectra were recorded on Bruker spectrometers equipped with a 7.0, 9.4, and 11.7 T UltraShield™ magnets operating, respectively, for ^{1}H at 300.1, 400.1, and 500.1 MHz; for ^{13}C at 75.5, 100.6, and 125.8 MHz. Standard Bruker room temperature probes were used. Chemical shifts are quoted in ppm as referenced to residual solvent peaks. ^{1}H spectra are reported as follows: δ (operating frequency, solvent): ppm (assignment, multiplicity, coupling constant(s), number of protons). ^{13}C spectra are reported as follows: δ (operating frequency, solvent): ppm (assignment). Resonance assignments were aided by DEPT (=Distortionless enhanced polarization transfer), COSY (=Correlation spectroscopy), HMBC (Heteronuclear multiple bond coherence), or HSQC (Heteronuclear single quantum correlation) experiments.

Infrared (IR) spectroscopy
Fourier transformed IR spectra were recorded from neat samples on a Perkin-Elmer Spectrum One FT-IR spectrophotometer fitted with an attenuated total reflectance sampling accessory. Absorption maxima are reported in wavenumbers (cm^{-1}).

High-resolution mass spectrometry (HRMS)
Analytical masses were recorded on an LCT Premier orthogonal acceleration time-of-flight or a Micromass quadrupole-time-of-flight mass spectrometers from Waters.

Liquid chromatography-mass spectrometry (LCMS)
Analytical LCMS chromatograms were obtained using a Supelcosil ABZ+PLUS (alkylamide) column (4.6 mm x 33 mm, 3 µm), employing an Agilent 1200 series LC instrument coupled with a Waters mass spectrometry system, combining an ESCi multi-mode ionization source and a Micromass ZQ single quadrupole detector. The data was processed using Waters MassLynx 4.1. LCMS chromatograms were additionally monitored by UV absorbance using a diode array with detection at a wavelength range of 190-600 nm.

High-performance liquid chromatography (HPLC)
HPLC was run on an Agilent 1260 Infinity, an Agilent 1100 or a Jasco LC-2000 series instruments using for analytical chromatograms a Supelcosil ABZ+PLUS (alkylamide) (4.6 mm x 150 mm, 3 µm) or a Vydac 218TP (C_{18}) (4.6 mm × 250 mm, 10 µm) columns and eluting with linear A:B gradients at a flow rate of 1.5 mL/min. If not stated otherwise, eluent A: 97% H_2O, 3% acetonitrile, 0.1 % 2,2,2-trifluoroacetic acid (TFA), eluent B: 10% H_2O, 90% acetonitrile, 0.1 % TFA. Semi-preparative HPLC employed a Vydac 218TP (C_{18}) (22 mm × 250 mm, 10 µm) column, linear gradients of the same eluents, and a flow rate of 20 mL/min. HPLC was monitored by UV absorbance using a diode array with detection at a wavelength range of 200-650 nm.

Chemical nomenclature and atom numbering
Systematic compound names are those generated by Perkin-Elmer ChemBioDraw Ultra 13.0 following the IUPAC conventions. The numbering of atoms for spectral assignment is consistent with the IUPAC names.

Synthesis of building blocks (2) and (3)

4,4'-cyclopent-1-ene-1,2-diylbis(5-methylthiophene-2-carboxylic acid) (9)

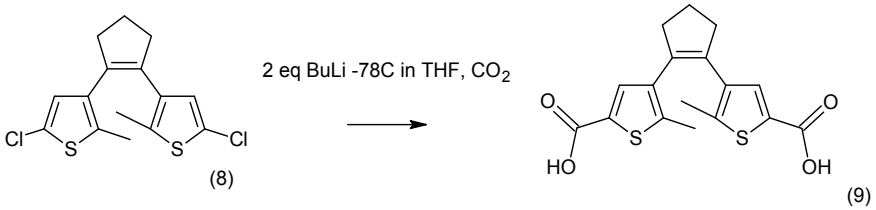

(8) (9)

The dicarboxylic acid **9** was synthesized starting from the 2,2'-dichloroderivative **8**; synthesis of the latter was described elsewhere [S1]. Compound **8** (14.4 g, 0.044 mol) was dissolved in dry THF (300 mL) in 3-necked round-bottom 1 L flask under argon and cooled to -78 °C. Afterward, 2.5 M BuLi (=n-butyllithium) in hexane (2.2 equiv, 38,5 mL, 0.096 mol) was added dropwise under stirring. After the addition of BuLi was completed, the reaction mixture was warmed to 0 °C within 30 min and kept at this temperature for another 10 min. A yellowish precipitate of the intermediate was formed. The mixture was cooled again to -78 °C, and dry CO_2 (15 g) was added. After warming to ambient temperature, the mixture was poured into water (500 mL), acidified with 2N aqueous HCl till pH 5 and extracted with ethyl acetate (2 x 200 mL). The organic phase was decreased under reduced pressure to a volume of 50-70 mL and left standing for crystallization of the crude product. After a few hours, the product was filtered as a white powder (12 g, 78%) and used in further steps without additional purification. **^{1}H NMR** (300 MHz, DMSO-d_6): δ = 1.91 (s, 6H, $2CH_3$), 1.98 (m, 2H, CH_2), 2.77 (t, 4H, $2CH_2$), 3.36 (s, broad, 2H, 2OH), 7.42 (s, 2H, 2CH). The spectral data are in full agreement with the literature [S1].

4,4'-cyclopent-1-ene-1,2-diylbis(5-methyl-N-(prop-2-yn-1-yl)thiophene-2-carboxamide) (2)

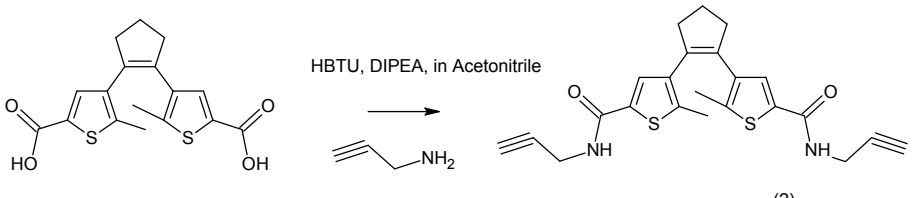

(9) (2)

The dicarboxylic acid **9** (1 g, 0.00287 mol) and DIPEA (4 equiv, 2 mL, 0.0155 mol) were dissolved in acetonitrile (20 mL) at ambient temperature. HBTU (=2-(1H-benzotriazol-1-yl)-1,1,3,3-tetramethyluronium hexafluorophosphate, 2.2 equiv, 2.4 g, 0.00631 mol) was added to the solution, and the resulting mixture was stirred for 2 min, then combined with 2-propynylamine (3 equiv, 0.316 g, 0.00861 mol). The reaction mixture was stirred overnight and then poured into 5% aqueous citric acid (200 mL). The product was extracted with ethyl acetate (3 x 100 mL). The combined organic extracts were washed with water (2 x 100 mL), dried over Na_2SO_4, and the organic solvents were removed in vacuum. The obtained product was triturated with ethyl acetate (10 mL) and filtered. White crystals (1.03 g, 85%). **^{1}H NMR** (400 MHz, DMSO-d_6): δ =.79 (H21+H22, t, J = 5.6 Hz, 2H), 7.57 (H8+H12, s, 2H), 3.99 (H24+H26, dd, J = 5.6, 2.6 Hz, 4H), 3.14 (H28+H29, t, J = 2.6 Hz, 2H), 2.77 (H1+H4, t, J = 6.7 Hz, 4H), 2.03 (H2, qt, J = 6.7 Hz, 2H), 1.84 (H16+H17, s, 6H). **^{13}C NMR** (101 MHz, DMSO-d_6): δ = 160.6 (C18+C19), 139.38 (C10+C14), 136.14 (C6+C11), 134.99 (C7+C13), 134.11 (C3+C5), 129.34 (C8+C12), 81.14 (C27+C25), 73.11 (C28+C29), 38.24 (C1+C4), 28.25 (C24+C26), 22.28 (C2), 14.25 (C16+C17). **HRMS**, calculated for $C_{23}H_{22}N_2O_2S_2$: 422.1123; found: 422.1120.

4,4'-cyclopent-1-ene-1,2-diylbis(N,5-dimethyl-N-(prop-2-yn-1-yl)thiophene-2-carboxamide) (3)

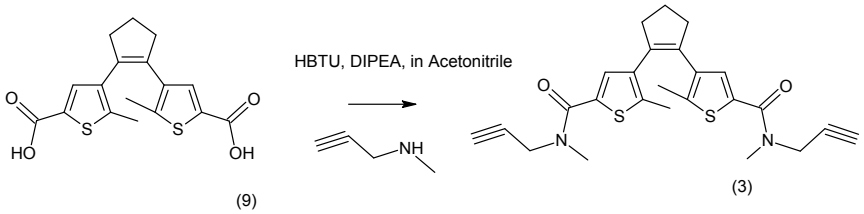

Synthesis of compound **3** was performed analogously to that of compound **2**. Crude **3** was obtained as a yellow oil and further purified by column chromatography on silica gel using hexane/ethyl acetate (1:1 vol.) mixture as eluent (0.85 g, 70%). **^{1}H NMR** (400 MHz, $CDCl_3$): δ = 7.11 (H8+H12, s, 2H), 4.21 (H24+H26, broad s, 4H), 3.14 (H30+H31, broad s, 6H), 2.84 – 2.74 (H1+H4 and H28+H29, m, 6H), 2.12 – 2.02 (H2 and H16+H17, m, 8H). **^{13}C NMR** (101 MHz, $CDCl_3$): δ = 163.96 (C18+C19), 139.83 (thiophene), 135.70 (thiophene), 135.18 (C3+C5), 133.06 (thiophene), 131.30 (C8+C12), 78.68 (C28+C29), 72.91 (broad due to slow amide bond rotation, C25+C27), 38.74 (C30+C31), 38.12 (C1+C4), 35.29 (broad due to slow amide bond rotation, C24+C26), 23.07 (C2), 14.54 (C16+C17). **HRMS**, calculated for $C_{25}H_{26}N_2O_2S_2$: 450.1436; found: 450.1431.

The spectra for the novel compounds are shown in **Figures S1-S12**.

Figure S1. ^{1}H NMR spectrum of 2

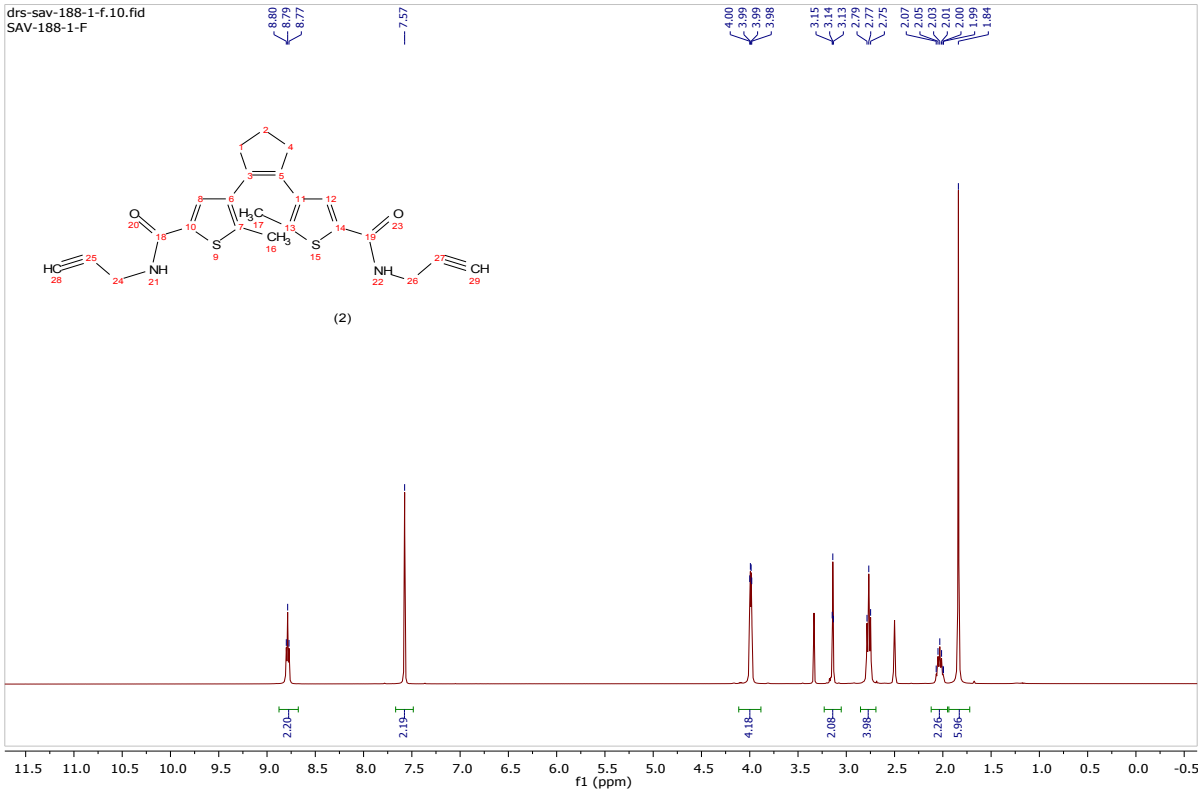

Figure S2. ^{13}C NMR spectrum of 2

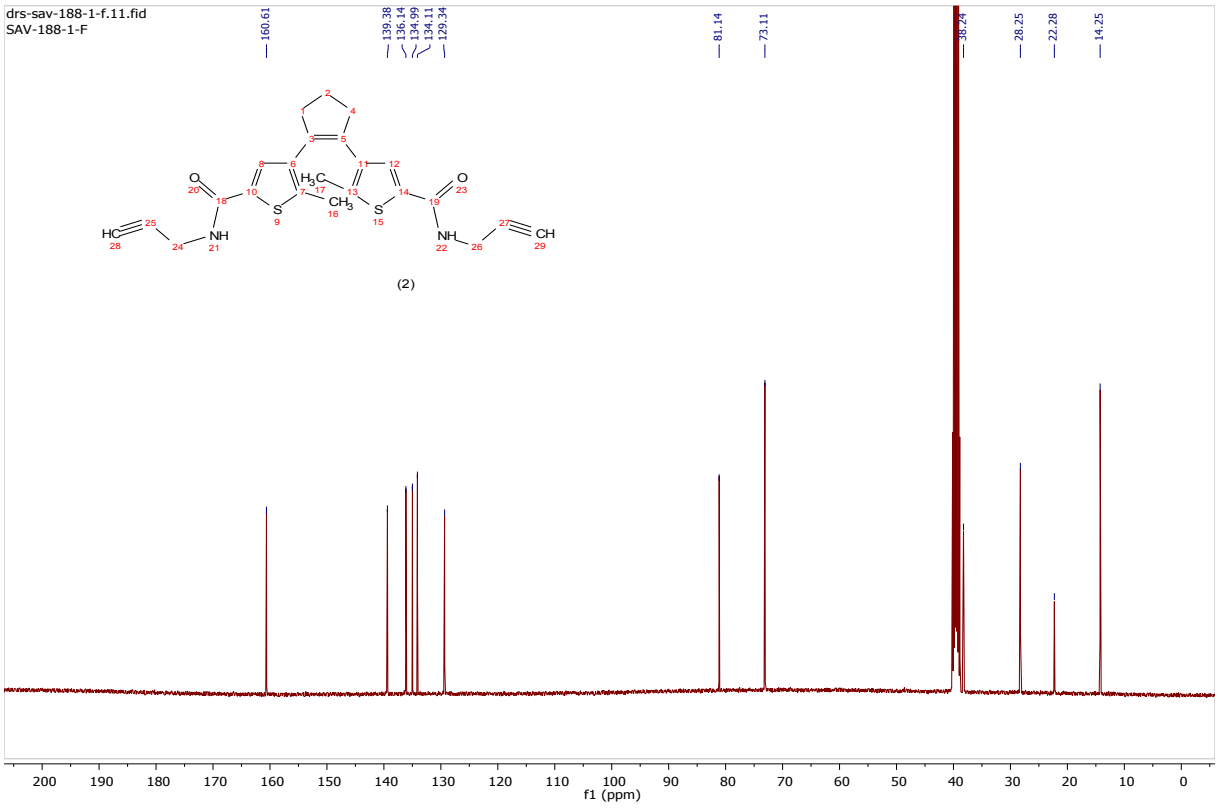

Figure S3. DEPT-135 ^{13}C NMR spectrum of 2

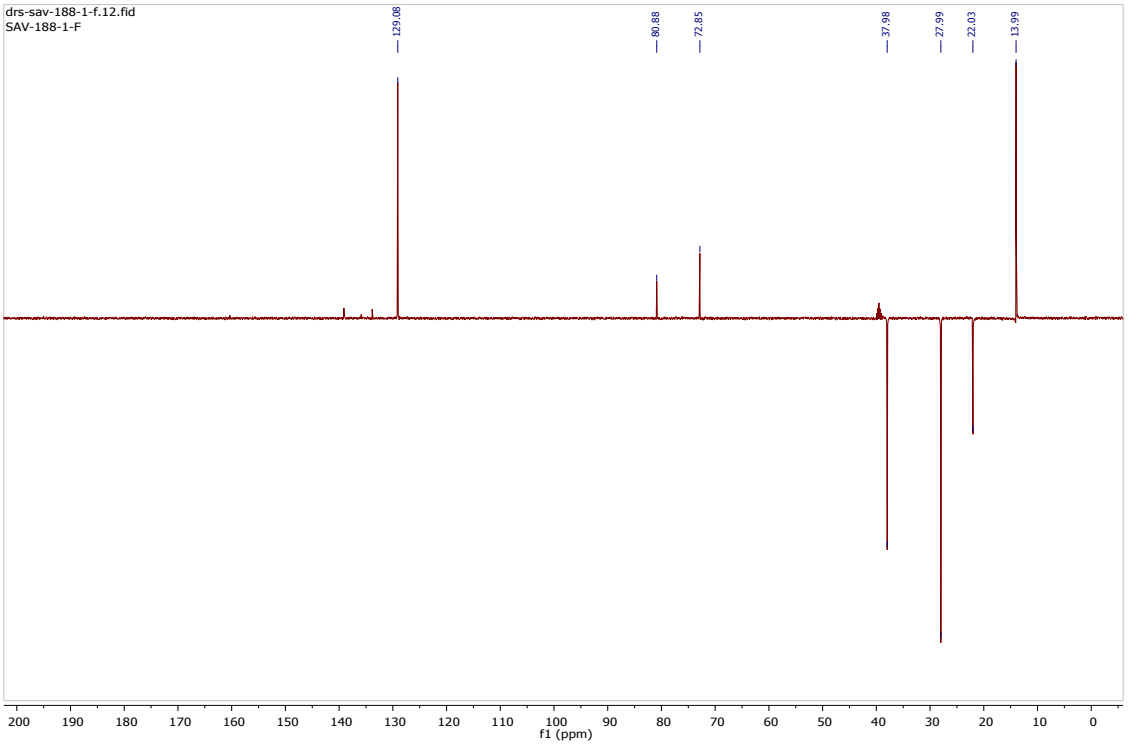

Figure S4. ^{1}H-^{1}H COSY NMR spectrum of 2

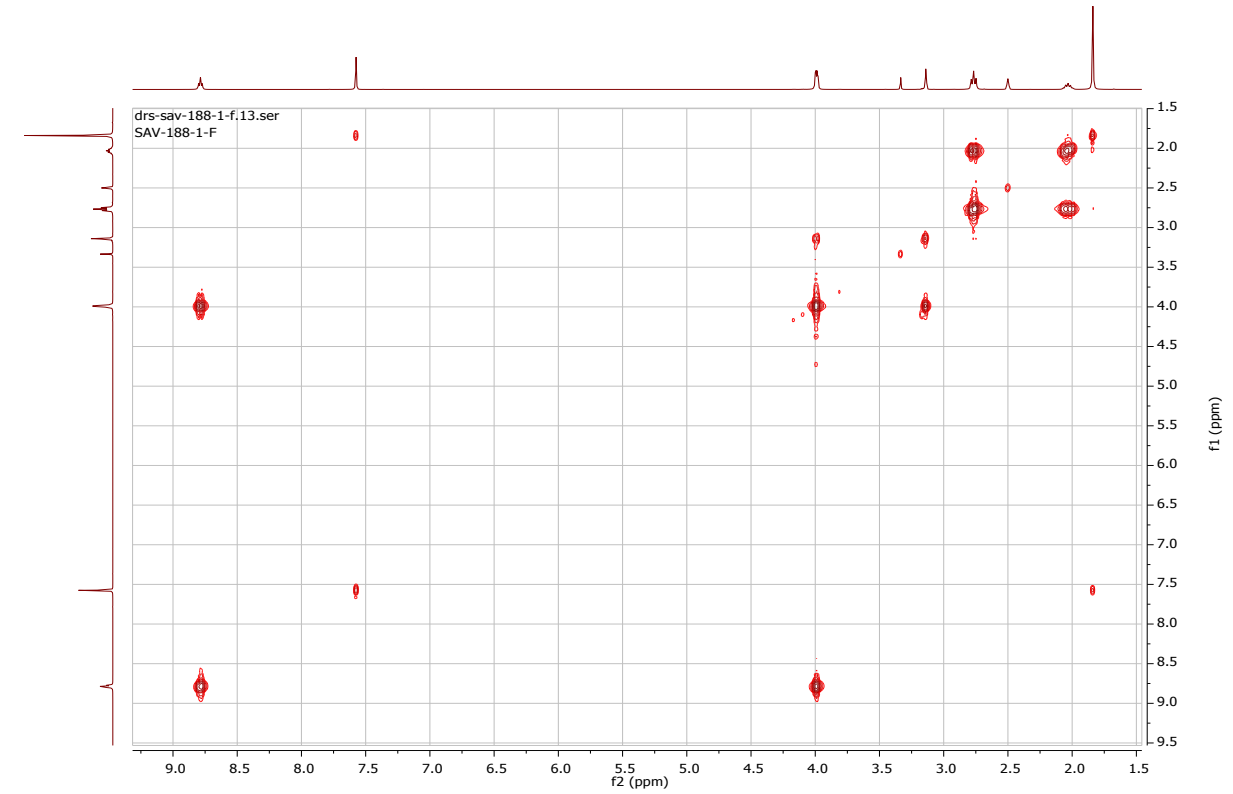

Figure S5. ^{13}C-^{1}H HSQC NMR spectrum of 2

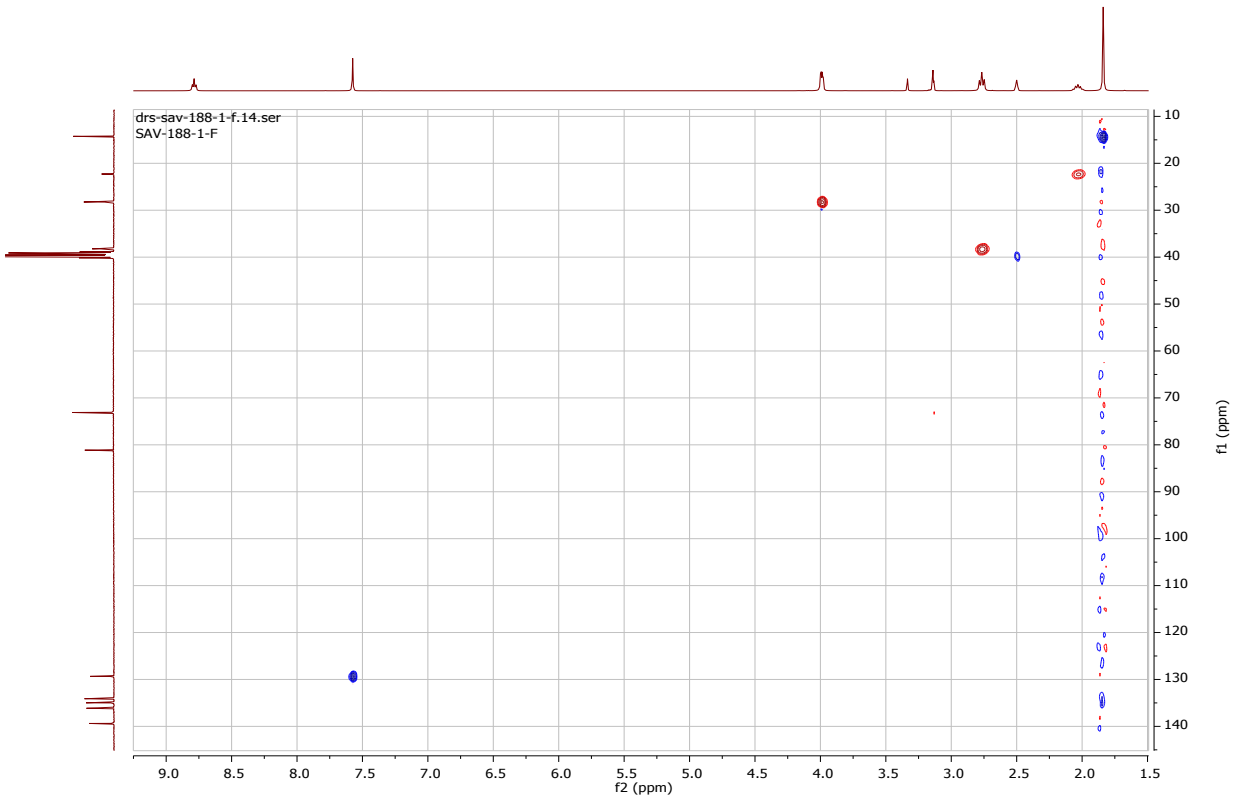

Figure S6. ^{13}C-^{1}H HMBC NMR spectrum of 2

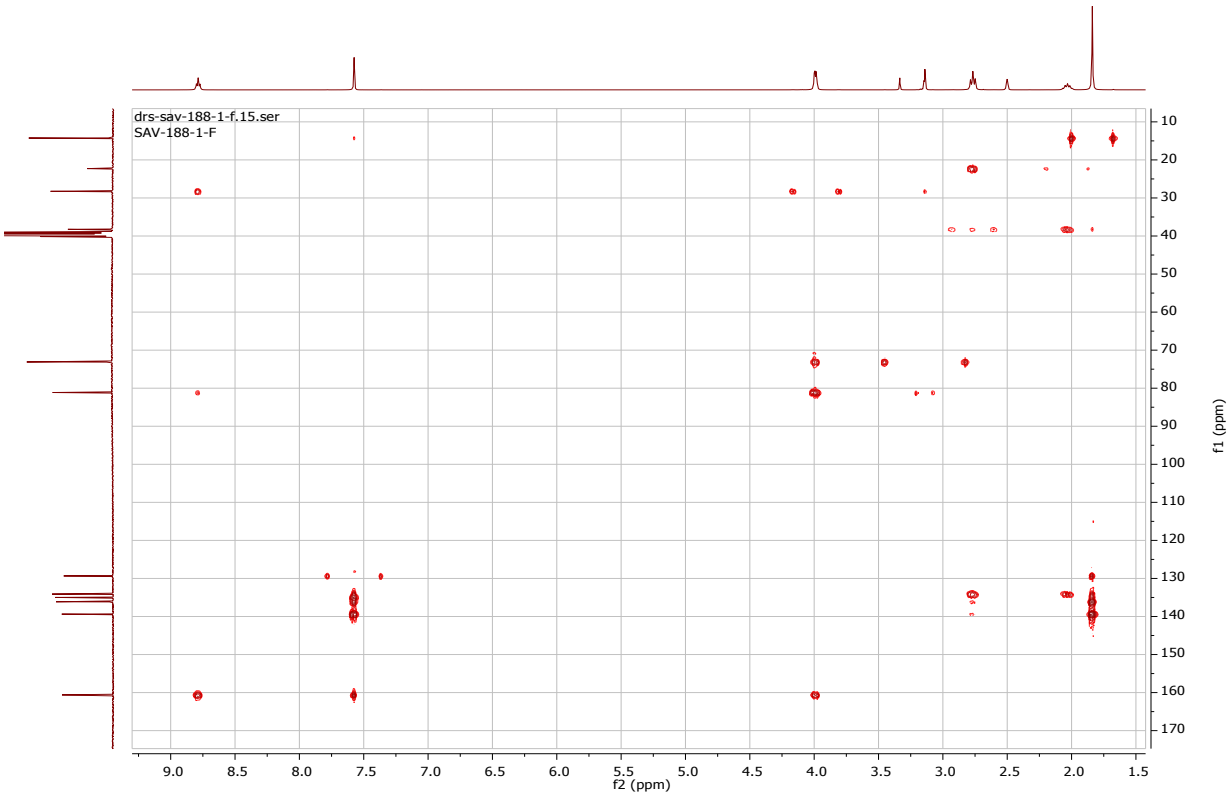

Figure S7. ^{1}H-NMR spectrum of 3

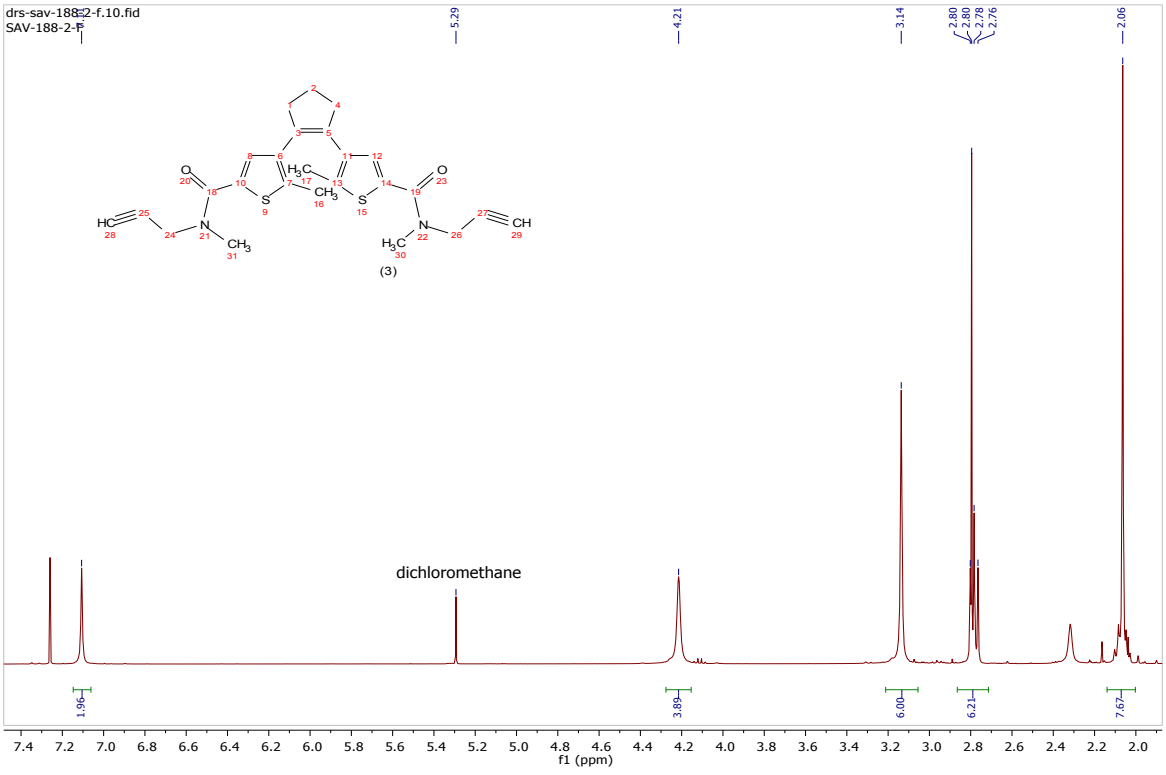

Figure S8. ^{13}C-NMR spectrum of 3

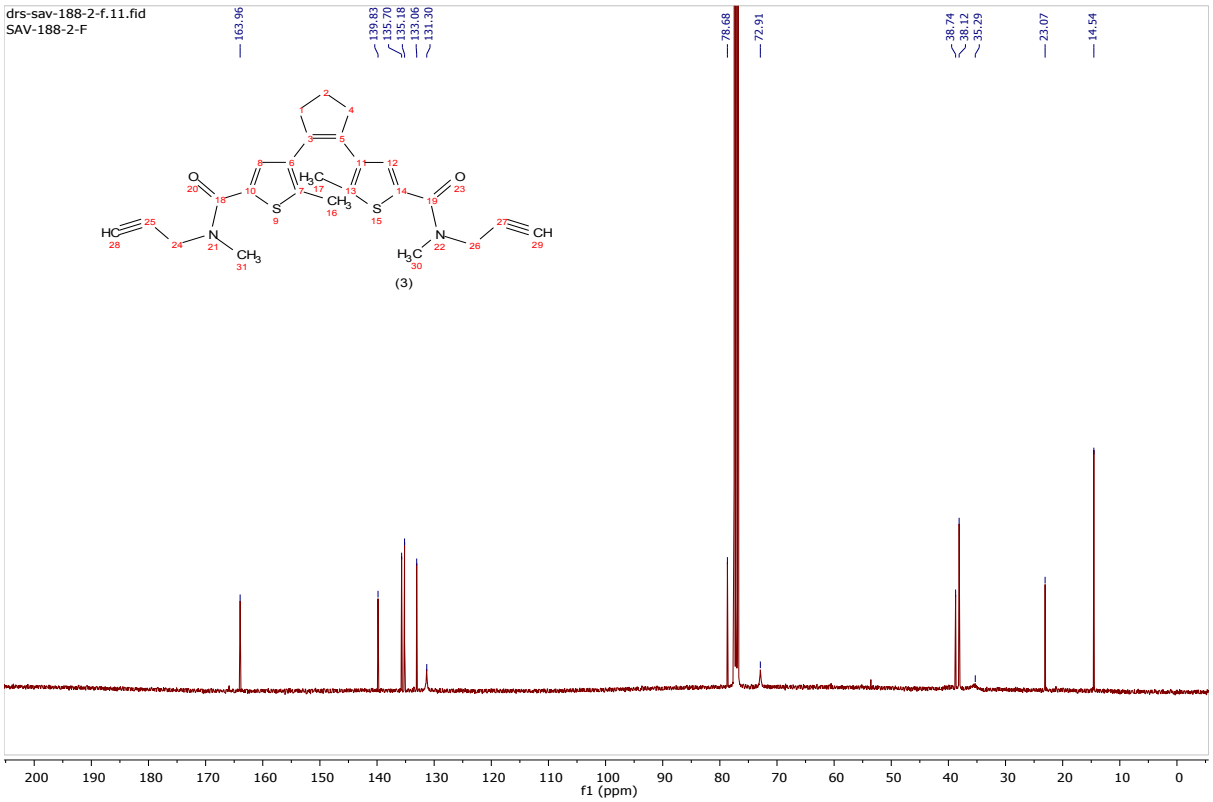

Figure S9. DEPT-135 ^{13}C NMR spectrum of 3

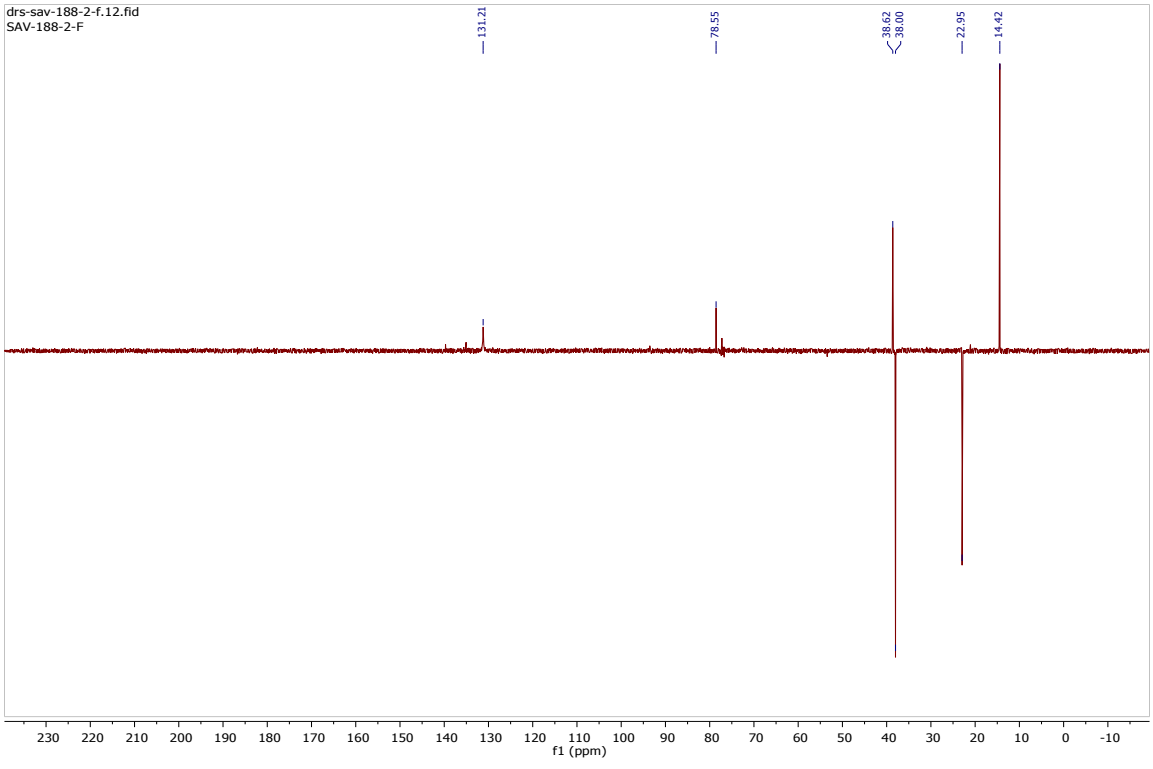

Figure S10. ^{1}H-^{1}H COSY NMR spectrum of 3

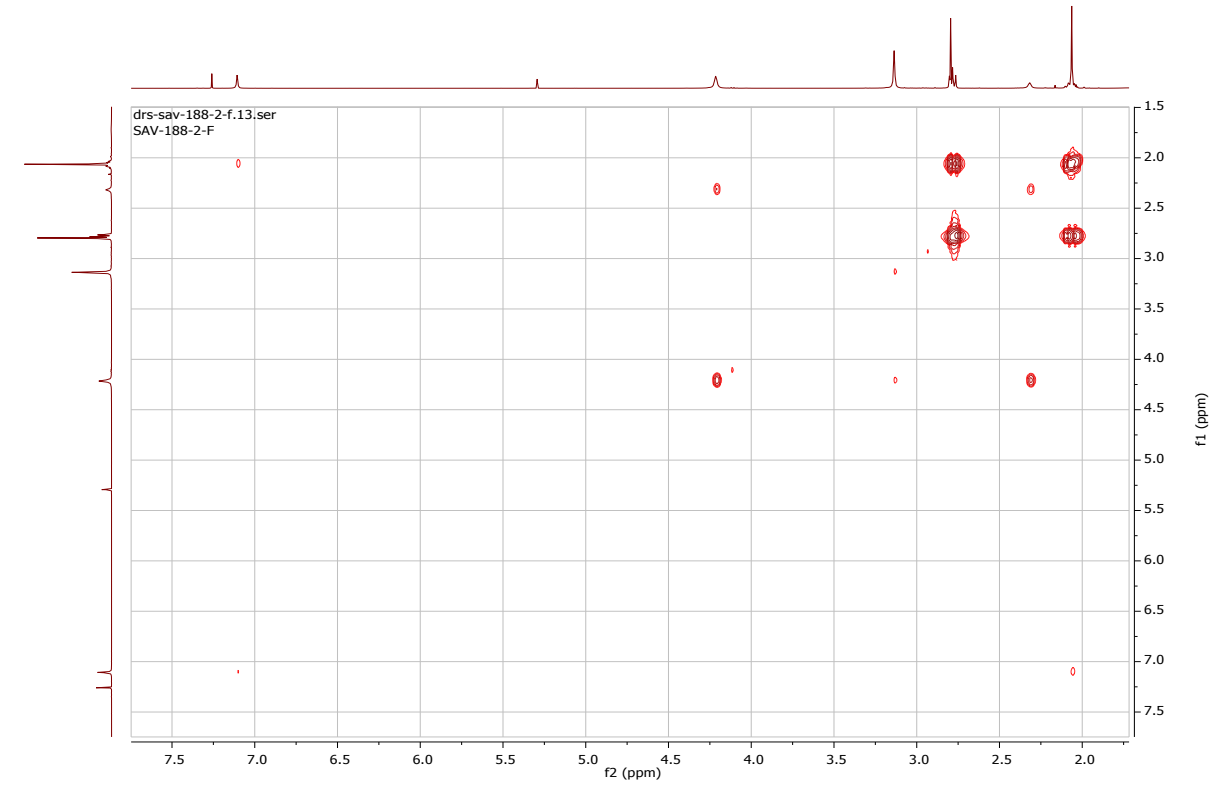

Figure S11. ^{13}C-^{1}H HSQC NMR spectrum of 3

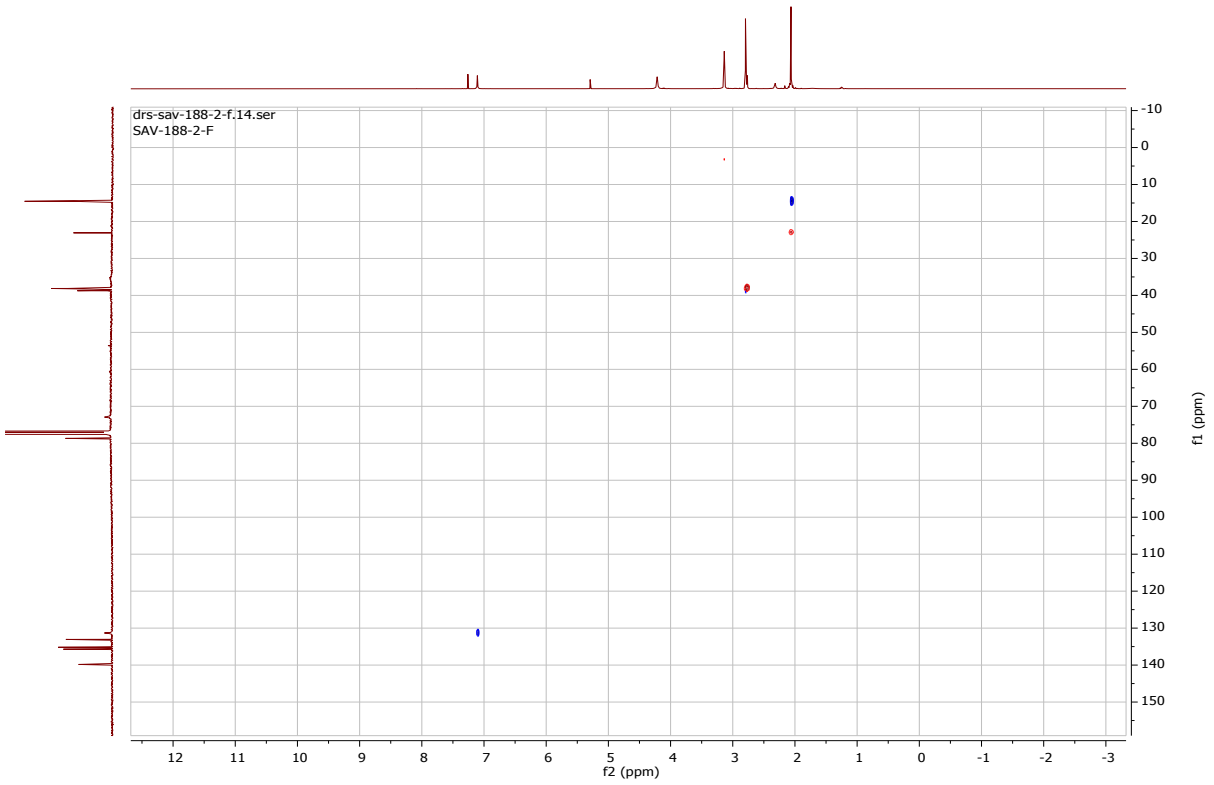

Figure S12. ^{13}C-^{1}H HMBC NMR spectrum of 3

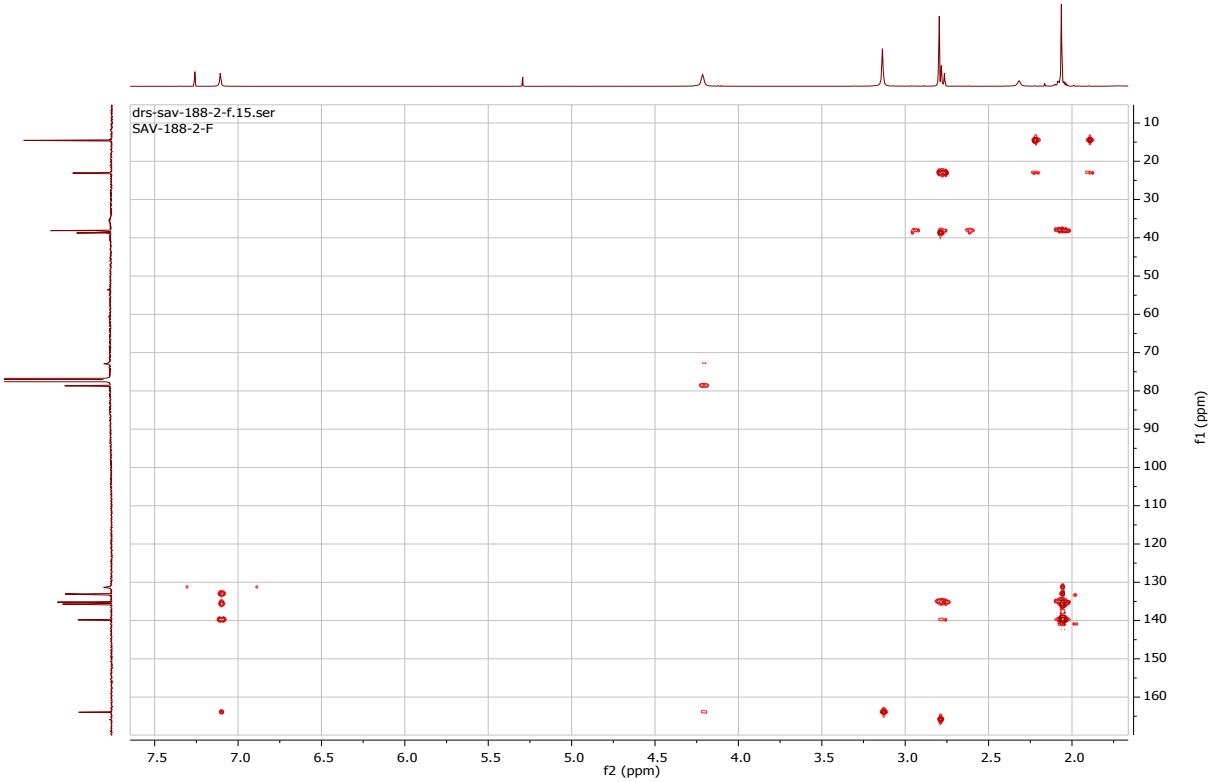

General procedure for the synthesis of the linear peptide precursors 1a,b

Standard Fmoc (9-fluorenylmethoxycarbonyl) strategy solid-phase peptide synthesis protocols and commercially available reagents were used. Rink amide 4-methylbenzhydrylamine resin preloaded with an appropriate amino acid with the loading of 0.67 mmol/g (150 mg, 1 equiv) was used. Coupling of the amino acids was performed using the following molar ratios of the reagents: (i) Fmoc-amino acid (4 equiv), HOBt (=1-hydroxybenzotriazole, 4 equiv), HBTU (3.9 equiv), DIPEA (8 equiv) - for natural amino acids; (ii): Fmoc-amino acid (2 equiv), HOBt (2 equiv), HATU (=N-[(7-Aza-1H-benzotriazol-1-yl)(dimethylamino)-methylene]-N-methylmethanaminium hexafluorophosphate N-oxide, 1.95 equiv), DIPEA (4 equiv) - for non-natural amino acids, Fmoc-Orn(N_3)-OH and Fmoc-Lys(N_3)-OH. The coupling time in all cases was 40 min. N-Fmoc deprotection was carried out by treating the resin with 20% piperidine in dimethylformamide for 20 min. The N-terminus acetylation was done with acetic anhydride (3 equiv) and DIPEA (5 equiv) in dimethylformamide. After completing the synthesis, the resin was washed with dichloromethane and dried under vacuum for 24 h. The peptides were cleaved from the resin with a cleavage cocktail (TFA, triisopropylsilane, and water, 92.5:2.5:5 vol., 10 mL, 60 min). The volatile products were blown off from the filtered solutions by argon. Residual materials were dissolved in an acetonitrile-water (1:1) mixture and lyophilized. The crude peptides were purified on a semi-preparative C_{18} column with a linear A:B gradient of 5% B/min slope. The purity of the peptides was determined on an analytical C_{18} column with a linear A:B gradient of 1% B/min slope.

General procedure for the synthesis of peptides 4-7 (open forms) based on Cu-catalysed "double-click" protocol [S2]

Corresponding precursor (**1a** or **1b**, 0.01 mmol) was dissolved in 100 mL of 50% *t*-BuOH/H_2O mixture, then a solution of a DAE derivative (**2** or **3**, 0.011 mmol) in acetonitrile (0.5 mL), a solution of THPTA ligand (=tris(3-hydroxypropyltriazolylmethyl)amine, 0.01 mmol) in acetonitrile (0.1 mL), and a $CuSO_4x5H_2O$ solution in water (0.01 mmol in 0.1 mL) were added. The solution was degassed by sparging with argon for 10 min, after which a solution of sodium ascorbate (0.03 mmol in 0.1 mL H_2O) was added, and the reaction mixture was vigorously stirred under argon atmosphere for 1-3 days. The reaction was monitored by an analytical HPLC and LCMS. After completion of the reaction, the mixture was freeze-dried and subjected to a preparative HPLC. IR was used to confirm that the stapled peptides **4**-**7** (open forms) were not potential linear products with the same masses. Absorbance at ~2100 cm^{-1} was observed in the unstapled precursors **1a** and **1b** but not in the stapled peptides **4**-**7**, confirmed by the absence of unreacted azido groups.

Peptide **4,** yield 14 mg (70%); Peptide **5**, yield 12.9 mg (64%); Peptide **6**, yield 11.4 mg (56%); Peptide **7**, yield 11.1 mg (54%).

Typical HPLC and LCMS traces can be seen in the attached files (SI_Compound_7_Crude.pdf and SI_Compound_7_Purified.pdf, exemplified by compound 7)

HPLC analysis of peptides

The purity of the peptides was analyzed in both open and closed photoforms by analytical HPLC. The analysis was conducted on a C_{18} phase column (temperature 40 °C, flow rate 1.5 mL/min, gradient: 20% to 80% B in 20 min, slope 3% B/ min, eluent A: 97% H_2O, 3% acetonitrile, 0.1% TFA, eluent B: 10% H_2O, 90% acetonitrile, 0.1% TFA. The analysis confirmed >96% purity for both photoforms of each compound (**Figure S13**). The closed photoforms of the peptides eluted earlier than the corresponding open photoforms.

Figure S13. HPLC traces at 220 nm for the purified peptides 4-7

4 (Orn-NH) -open (top) and -closed (bottom) photoforms:

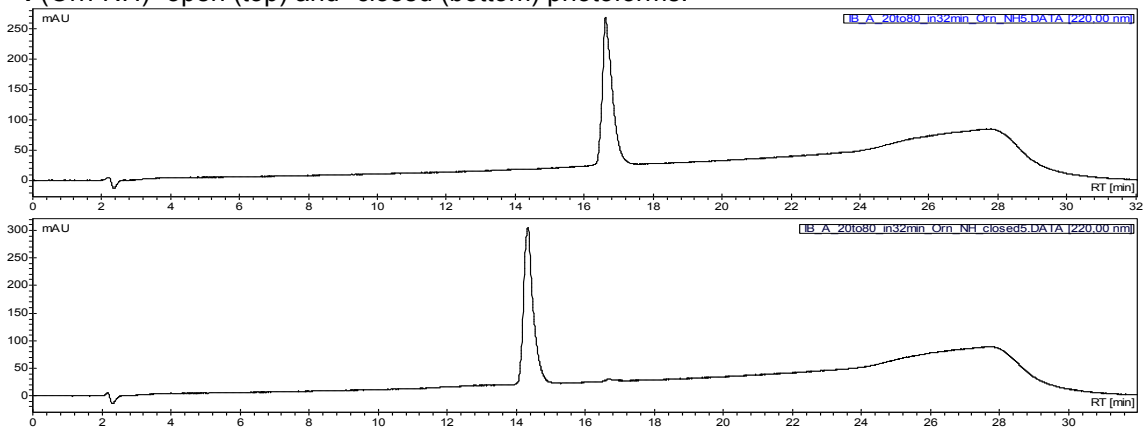

5 (Orn-NMe) -open (top) and -closed (bottom) photoforms:

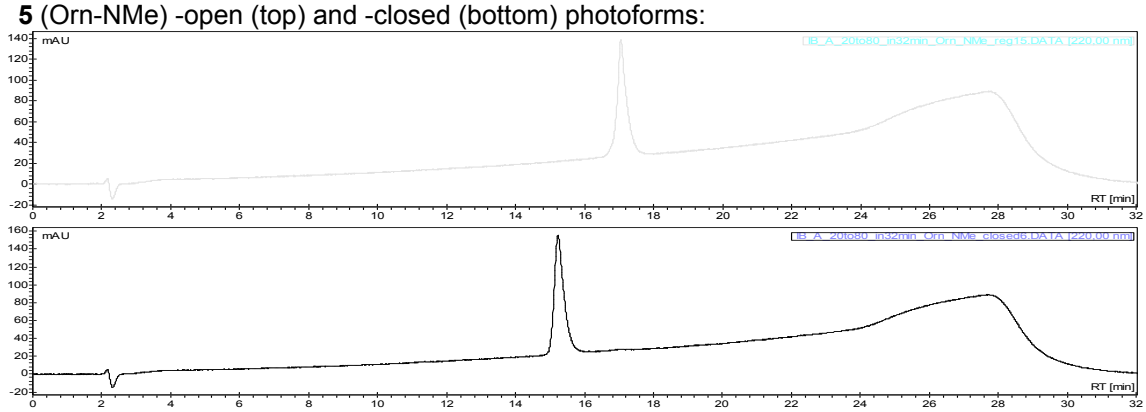

6 (Lys-NH) -open (top) and -closed (bottom) photoforms:

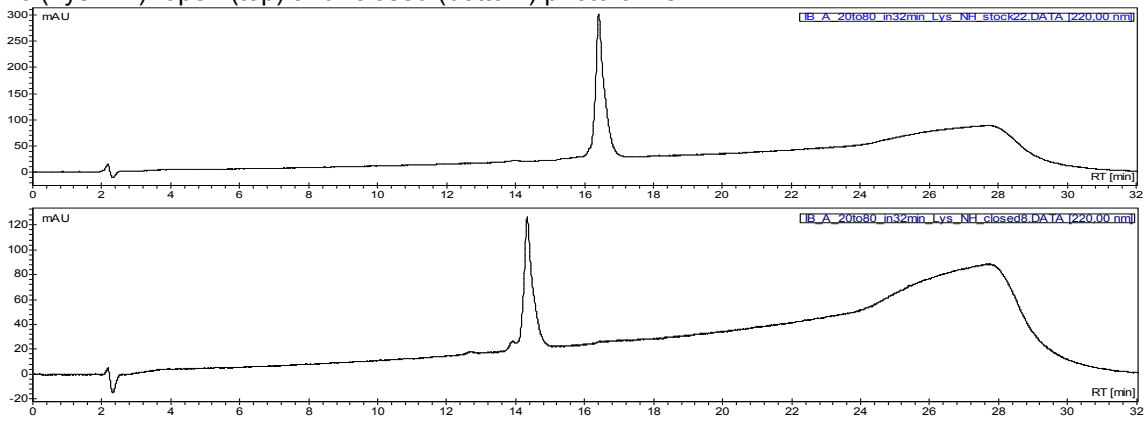

Figure S13. (continued)

7 (Lys-NMe) -open (top) and -closed (bottom) photoforms:

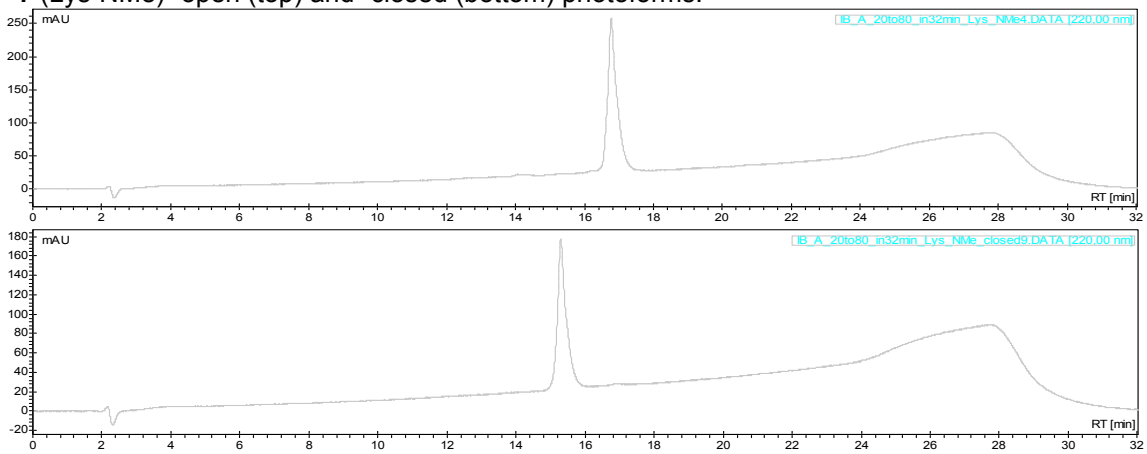

Mass spectrometry analysis of peptides

The identity of peptides was confirmed by matrix-assisted laser-induced desorption/ionization with time-of-flight detection (MALDI-TOF) mass spectrometry. The measurements were performed on a Bruker Autoflex III instrument using linear mode and positive ion polarity. The ions below 1200 Th were deflected. Bruker stainless steel target, dried-droplet deposition, and standard matrices for peptides were employed. **MALDI-TOF**: m/z for peptide **4**: 2001.95 (calculated $[M+H]^+$: 2001.29); **5**: 2050.95 (calculated $[M+H]^+$: 2030.34, $[M+Na]^+$: 2052.33); **6**: 2029.95 (calculated $[M+H]^+$: 2029.34); **7**: 2080.89 (calculated $[M+H]^+$: 2057.39, $[M+Na]^+$: 2080.39). The spectra were measured after peptide purification (i.e., for the open forms, see **Figure S14**) and after pure closed forms were produced by irradiation with visible light (data not shown). In all cases, high purity, photoconversion stability, and identity were confirmed.

Figure S14. MALDI-TOF mass spectra for the peptides 4-7 (closed forms)

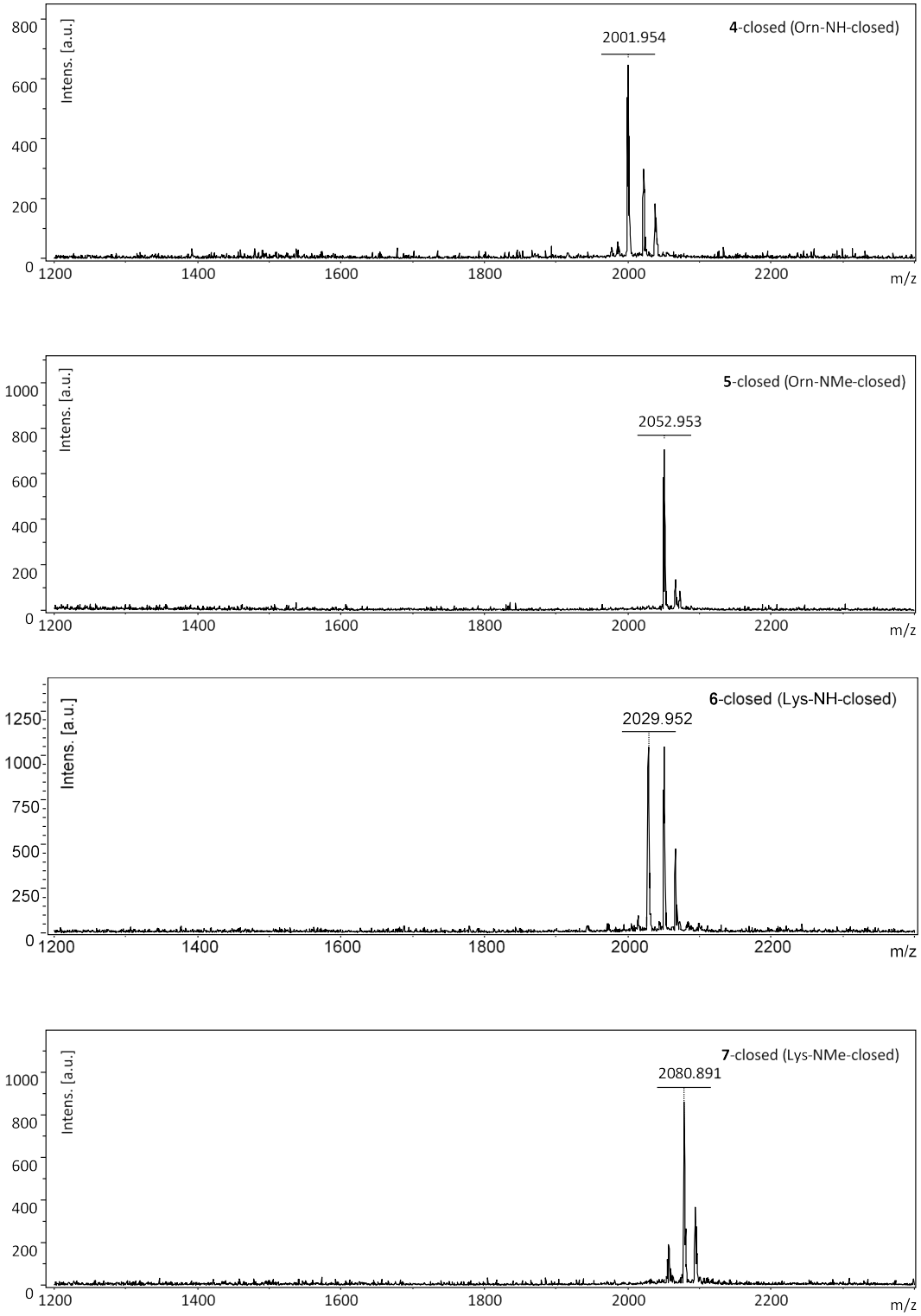

Tryptophan fluorescence quenching assays

Determination of the dissociation constant (K_d) for pDI/MDM2$^{6-125}$ complex

The peptide pDI (Ac-LTFEHYWAQLTS-NH_2) has one tryptophan residue which fluorescence can be used for the fluorescence quenching assay to determine the pDI/MDM$^{26-125}$ dissociation constant directly. The protein sequence (MDM2$^{6-125}$) has no tryptophan residues; seven tyrosine residues caused acceptable minor interference with the measurements.

The experiments were performed in a 10 mm quartz cuvette in 1x PBS buffer (=phosphate buffered saline, pH 7.4) in the presence of 0.005% Tween® 20 at 20 °C. The fluorescence was measured on a Fluorolog-3® instrument with the following parameters: 3 nm slit, excitation at 295 nm and emission monitored at 340-420 nm range (integration time 1 s) to measure the whole fluorescence spectrum or at a single wavelength 365 nm (integration time 16 s). The fluorescence intensity during titration with the protein was measured. A solution of pDI (1500 µL, 1 µM) was prepared in the cuvette and titrated with the MDM2$^{6-125}$ protein solution (10 µL each aliquot, 15 µM) followed by 5 min stirring before the fluorescence measurement at 365 nm. In total, 20 aliquots of the protein were added, resulting in 2 equiv to pDI. Blank experiments without the peptide were conducted to determine the background fluorescence of the MDM2$^{6-125}$ protein. The fluorescence intensity in the blank measurements was subtracted from the sample measurements to compensate for the protein background fluorescence. To account for the dilution during the titration, the intensity values were corrected by a factor α, where $\alpha = (1500+10*n)/1500$, n – the number of aliquots. Experimental results were plotted (**Figure S15**) using the following parameters: F_{max} – maximal fluorescence; F_{min} – minimal fluorescence; F_n – fluorescence after addition of n aliquots. Experimentally determined concentration of the complex (PL) was calculated using the equation: $[PL]_{experimental} = (1 - (F_n - F_{min})/(F_{max} - F_{min}))*P_T$ (P_T – total concentration of the protein (MDM2$^{6-125}$).

The dissociation constant K_d was obtained using the fit procedure assuming a single binding site model, with the following equation: $[PL]_{calculated} = (b - sqrt(b^2 - 4*c))/2$ ($c = P_T * L_T$; $b = K_d + P_T + L_T$; L_T – total concentration of the ligand (peptide pDI). The experiment was performed 3 times and an avarage value $K_d = 3 \pm 1$ nM was obtained [S3].

Determination of the apparent binding inhibition constant (K_i) for the pDI analogs 4-7 using pDI tryptophan fluorescence quenching

The photoswitchable pDI derivatives were not fluorescent despite having a tryptophan residue. This occurred due to the intramolecular quenching of tryptophan fluorescence by the diarylethene chromophore (in both photoforms). The fluorescent properties of the photoswitchable peptides were characterized as follows. First, for one of the peptides from the photoswitchable series (peptide **4**, (Orn-NH)) the fluorescence spectrum was measured (slit 3 nm, excitation 295 nm, emission 340-420 nm) at a concentration of 1 µM and compared with the fluorescent spectrum of pDI at the same concentration and experimental setting. The measurement confirmed that the **4**-closed has no fluorescence, while for the **4**-open form, weak residual intensity could be detected (around 5 % of the intensity of the original pDI). Additionally, a spectrum of **4** (open form) in the presence of 2 µM MDM2$^{6-125}$ (complete complexation of the peptide) was measured, which showed a slight change in the spectrum shape but still of very low intensity (**Figure S16**, MDM2$^{6-125}$ protein background was not subtracted). Nonetheless, because the peptide exhibits no fluorescence in the closed form, this method of quenching the intrinsic tryptophan fluorescence upon binding to the protein cannot be used to determine the equilibrium dissociation constant directly for the two photoforms of **4**.

Figure S15. Experimental data and fit curves for the determination of K_d of pDI binding to MDM2$^{6-125}$

Experiments 1, 2, and 3:

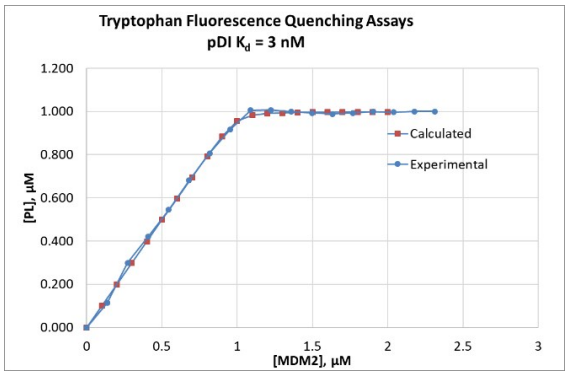

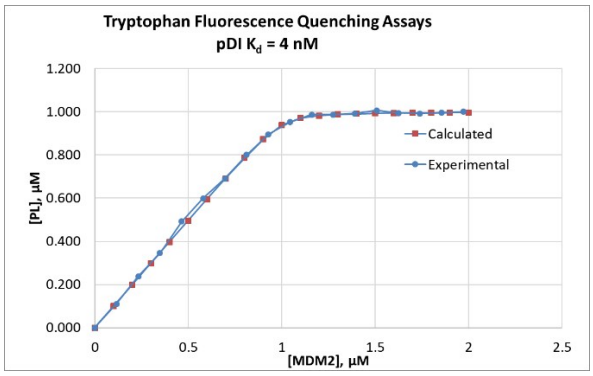

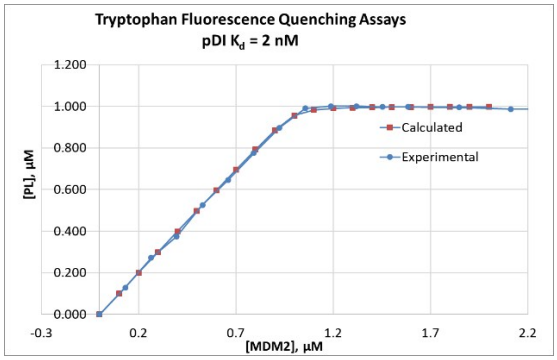

Fluorescence spectra of 1 µM pDI before (yellow trace) and after (blue trace) titration with 2 µM (final conc.) of the MDM2$^{6-125}$ protein:

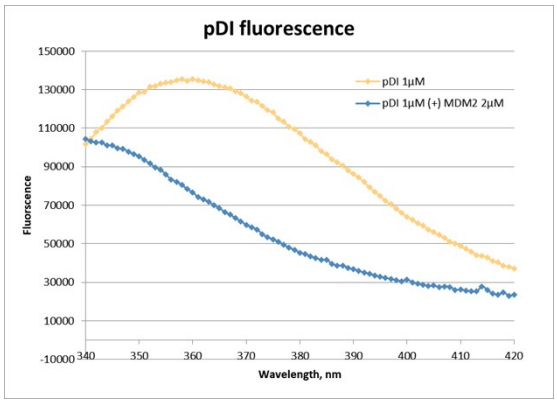

Figure S16. Fluorescence of the peptide 4 compared to that of pDI. The right panel is a 10x magnification of the full-scale left graph.

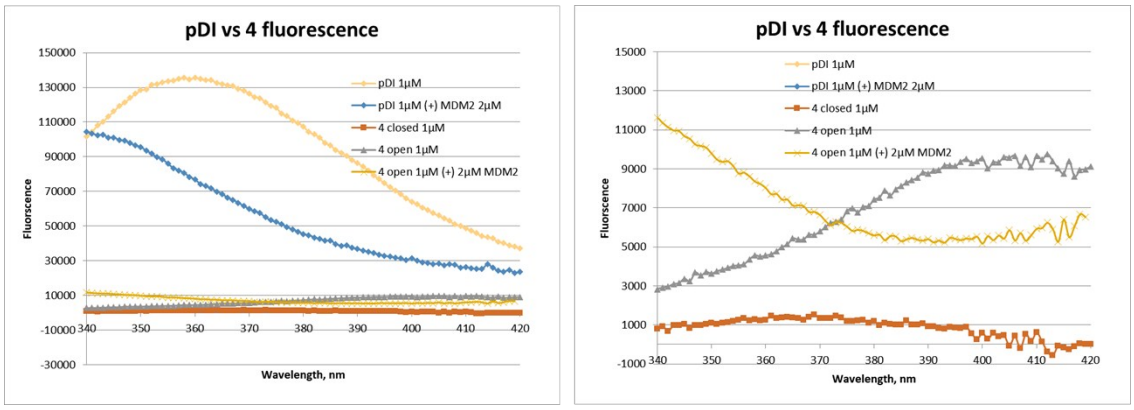

Therefore, to evaluate and compare the binding affinity for both photoforms of the peptides, a competitive binding assay with the pDI as a fluorescent reporter (for which the K_d was determined, **Figure S15**) was used. Similarly to the previous experiments, a 10 mm quartz cuvette and 1x PBS buffer (pH 7.4, 0.005% Tween20) at 20°C were used. The fluorescence was recorded with the following settings: slit 3 nm, excitation at 295 nm and emission at the range of 340-420 nm (integration time 1 s) to measure the whole fluorescence spectrum, or at a single wavelength 365 nm (integration time 16 s) to measure the fluorescence intensity during titration.

The experiment was carried out as follows: A solution of 1 μM pDI and 1 μM of a photoswitchable peptide was prepared (volume 1500 μL) in the cuvette. After recording the initial fluorescence, the solution was titrated with the $MDM2^{6-125}$ protein solution (15 μM) in 10 μL aliquots. After the addition of each aliquot of the protein followed by 5 min mixing, the fluorescence signal was recorded. To determine the background fluorescence of the protein, a blank experiment with no peptides in the solution was performed. The control experiment with only 1 μM pDI to check the absence of protein aggregation or precipitation (a known problem with the MDM2 protein) was also performed.

Data analysis: The background fluorescence of the $MDM2^{6-125}$ protein was subtracted, and a correction for the dilution during the titration was made by a factor α, where $\alpha = (1500+10*n)/1500$, n – number of aliquots. It is assumed that the photoswitchable peptides (pDI-Sw in the scheme below) bind to the $MDM2^{6-125}$ protein with a stoichiometry of 1:1 and the binding is competitive against the fluorescent pDI:

$$\begin{array}{ccc} \mathrm{MDM2} + \mathrm{pDI} & \rightleftharpoons & \mathrm{MDM2 \cdot pDI} \\ + & & \\ \mathrm{pDI\text{-}Sw} & & \\ \Updownarrow & & \\ \mathrm{MDM2 \cdot pDI\text{-}Sw} & & \end{array}$$

For both peptides, pDI and pDI-Sw, the equilibrium dissociation constants, K_{d1} and K_{d2}, according to the law of mass action can be written as shown in the equations (1) and (2). In the following equations [MDM2] – free concentration of the protein; $[MDM2]_T$ – total concentration of the protein; [pDI] and [pDI-Sw] – free concentrations of the peptides; $[pDI]_T$ and $[pDI\text{-}Sw]_T$ – total concentrations of the peptides; [MDM2·pDI] and [MDM2·pDI-Sw] – free concentrations of the respective peptide-protein complexes.

$$K_{d1} = \frac{[MDM2] * [pDI]}{[MDM2 \cdot pDI]} \quad (1)$$

$$K_{d2} = \frac{[MDM2] * [pDI\text{-}Sw]}{[MDM2 \cdot pDI\text{-}Sw]} \quad (2)$$

$$[MDM2] = \frac{K_{d1} * [MDM2 \cdot pDI]}{[pDI]} \quad (3)$$

$$[pDI] = [pDI]_T - [MDM2 \cdot pDI] \quad (4)$$

$$[MDM2] = \frac{K_{d1} * [MDM2 \cdot pDI]}{[pDI]_T - [MDM2 \cdot pDI]} \quad (5)$$

$$[MDM2]_T = [MDM2] + [MDM2 \cdot pDI] + [MDM2 \cdot pDI\text{-}Sw] \quad (6)$$

$$[MDM2 \cdot pDI\text{-}Sw] = [MDM2]_T - [MDM2] - [MDM2 \cdot pDI] \quad (7)$$

$$[pDI\text{-}Sw] = [pDI]_T - [MDM2 \cdot pDI\text{-}Sw] \quad (8)$$

$$[pDI\text{-}Sw] = [pDI]_T - [MDM2]_T + [MDM2] + [MDM2 \cdot pDI] \quad (9)$$

$$K_{d2} = \frac{[MDM2] * ([pDI]_T - [MDM2]_T + [MDM2] + [MDM2 \cdot pDI])}{[MDM2]_T - [MDM2] - [MDM2 \cdot pDI]} \quad (10)$$

The concentration [MDM2·pDI] is directly experimentally determined: $[MDM2 \cdot pDI]_{experimental} = (1 - (F_n - F_{min})/(F_{max} - F_{min}))*[pDI]_T$ where F_{max} – maximal fluorescence; F_{min} – minimal fluorescence; F_n – fluorescence after the addition of n aliquots. Thus, for each titration point, the free concentration of the protein, [MDM2], can be determined according to the equation (5). Next, the bound concentration of the pDI-Sw, [MDM2·pDI-Sw], is determined according to (7), and the free peptide concentration, [pDI-Sw], according to (9). These values put into the equation (2) gives the needed value for equilibrium dissociation constants K_{d2} (K_i) of the peptide pDI-Sw. K_i were calculated for seven titration points in the range 0.2-0.8 μM. The obtained results are illustrated in **Figure S17**.

Figure S17. Results of the competitive assays for the peptides 4-7. For each peptide the top panel represents experimental fluorescence readouts and calculated constants, bottom graphs plot experimentally measured concentrations of [MDM2·pDI] and calculated (equations (7) and (8)) concentrations of [pDI-Sw] and [MDM2·pDI-Sw] for an "open" photoform (bottom left) and for respective "closed" isomer (bottom right) throughout titration with the protein.

4 (Orn-NH)

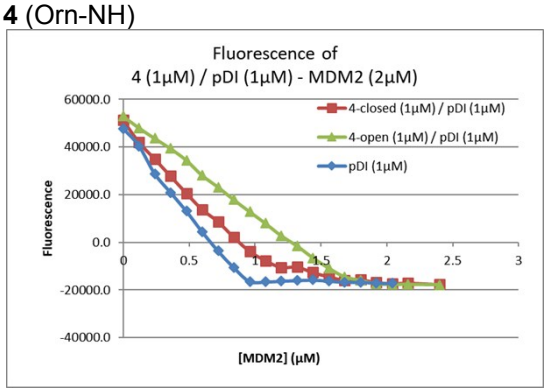

K_i (**4**-open) = 4 ± 0.6 nM

K_i (**4**-closed) = 33 ± 3.9 nM

Ratio = 8.3

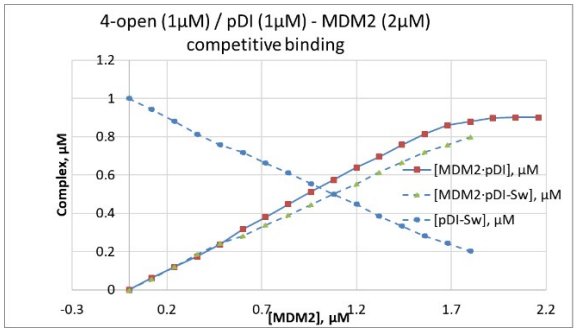

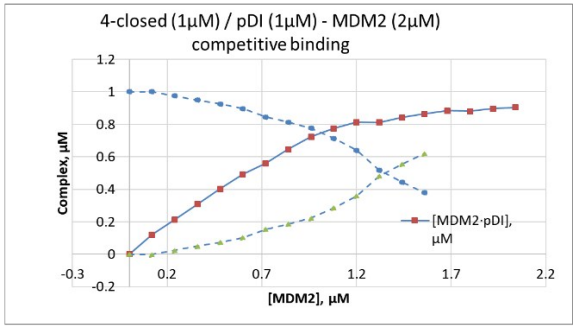

5 (Orn-NMe)

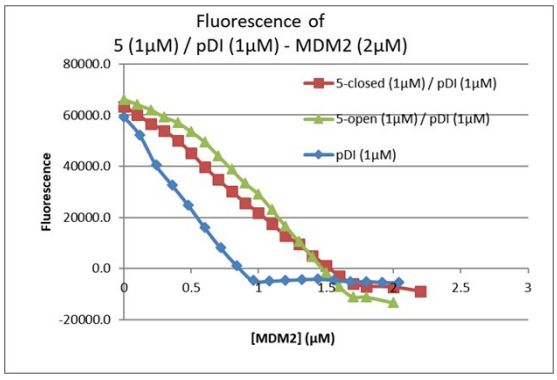

K_i (**5**-open) = 0.8 ± 0.1 nM

K_i (**5**-closed) = 2 ± 0.3 nM

Ratio = 2.5

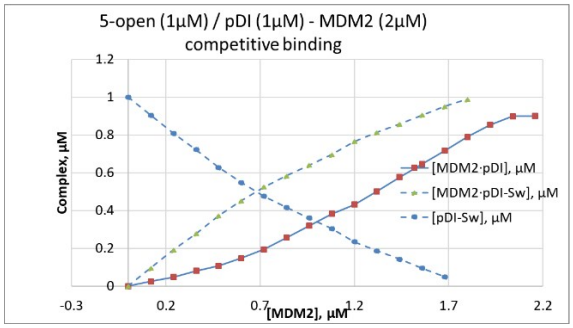

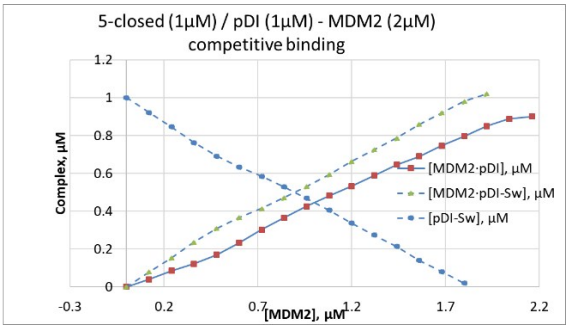

Figure S17. (continued)

6 (Lys-NH)

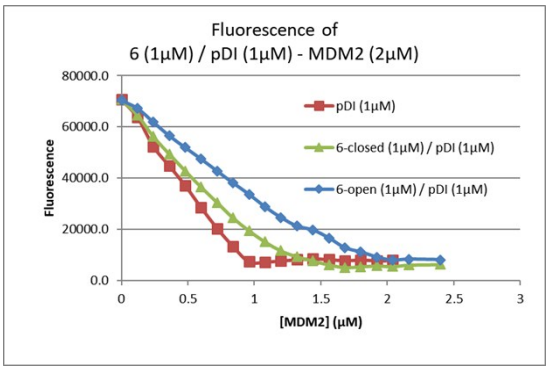

K_i (**6**-open) = 4.9 ± 0.55 nM

K_i (**6**-closed) = 26.8 ± 4.6 nM

Ratio = 5.5

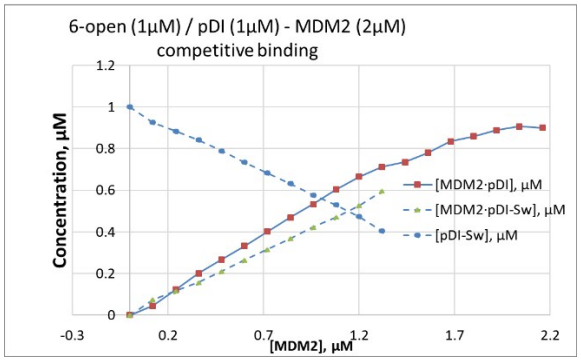

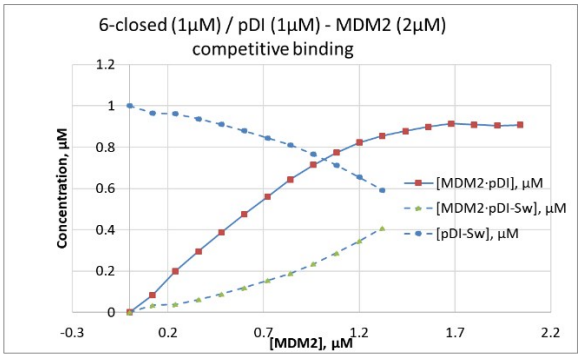

7 (Lys-NMe)

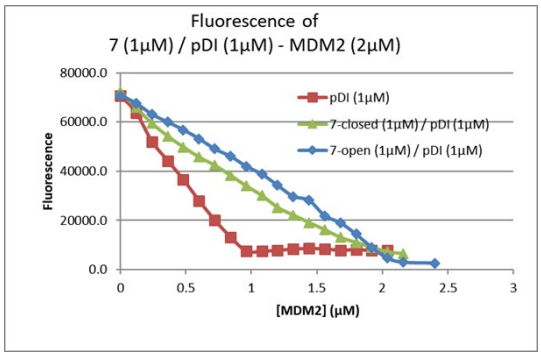

K_i (**7**-open) = 1.9 ± 0.2 nM

K_i (**7**-closed) = 7.2 ± 1.6 nM

Ratio = 3.8

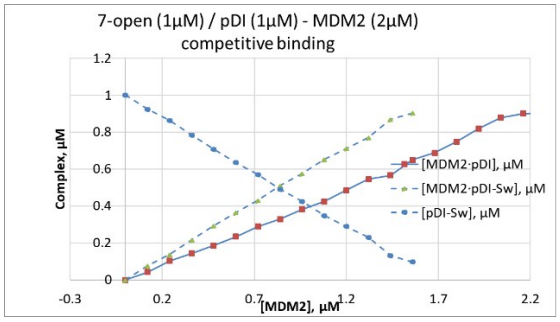

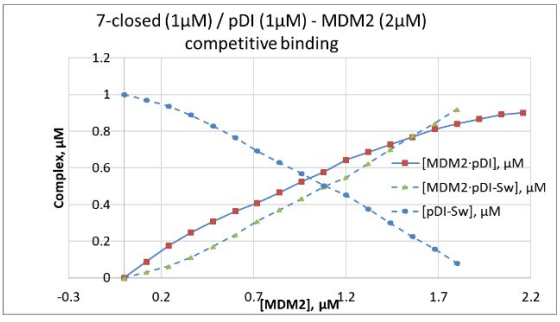

Competitive fluorescence polarization (FP) assay

This assay was based on an experiment we previously described in the literature [S4], with a change in fluorophore on the FP tracer from 5-FAM to 5-TAMRA. Stock solutions of peptides in dimethyl sulfoxide (DMSO, 10 mM) were diluted in assay buffer (1 × PBS + 0.01% Tween® 20 + 3% DMSO) to the highest concentration of 10 μM, then 1.6-fold serial dilutions were made to give a 16-point dose-response curve. A stock solution of FP tracer (10 mM) in DMSO and MDM2$^{6\text{-}125}$ was prepared in assay buffer to concentrations of 100 nM and 190 nM, respectively (final assay concentrations of 50 and 95 nM). Dilutions of peptides (20 μL) and FP tracer:MDM2$^{6\text{-}125}$ complex (20 μL) were added to a 384-well plate and incubated at 25°C for 30 minutes. The negative controls used assay buffer in place of a peptide, whilst the positive control was assay buffer in place of MDM2$^{6\text{-}125}$ and peptide. Experiments were conducted in two independent experiments, each in triplicate. Fluorescence polarisation was measured using a BMG Clariostar plate reader. K_i values were calculated by using a non-linear least-squares analysis fitting to the equations which have been previously described for binding with receptor depletion, and quoted with the standard error [S4]. Corresponding titration data and fit curves are shown in **Figure S18**.

Figure S18. Competitive FP inhibition curves for peptides (top, 5-open; middle, 6-open; bottom, 7-open)

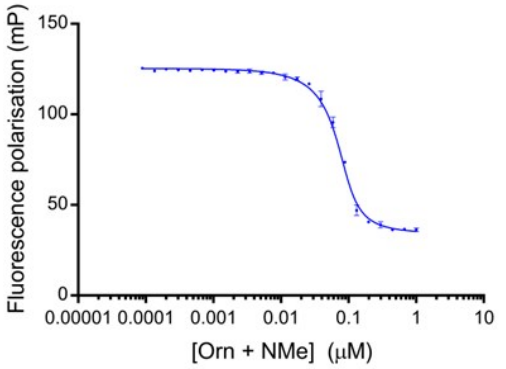

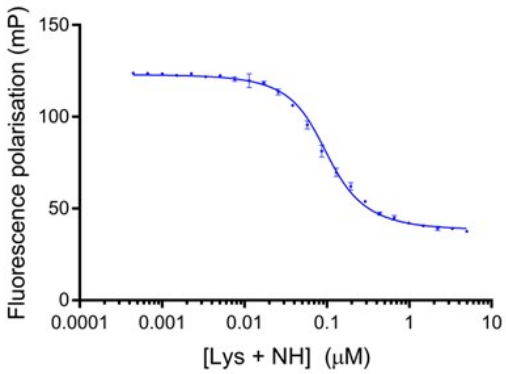

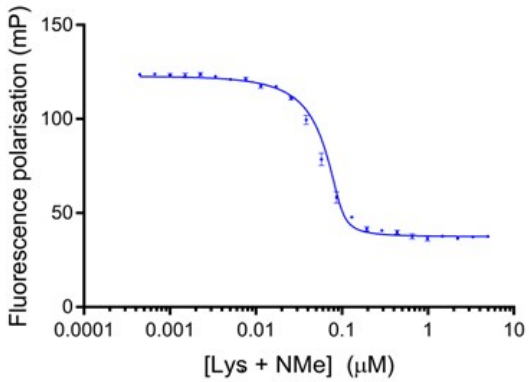

Isothermal titration calorimetry (ITC)

Measurements were performed on a Nano ITC Low Volume (TA Instruments) device. All experiments were done in phosphate-buffered saline (1x, pH 7.4) with 0.005% Tween® 20 at 25 °C. Peptides in PBS buffer at the concentration 16.6 μM in the calorimeter cell (total volume 170 μL) were titrated with the MDM2$^{6\text{-}125}$ protein dialyzed into the same buffer (97 μM, syringe volume 50 μL). The titration experiments were performed with an initial 1 μL injection followed by twenty-two 2 μL injections with 200 s spacing and 250 rpm mixing. Each experiment was repeated twice, and individual peptide results were reproducible. The obtained binding isotherms were fitted by a non-linear regression using a single-site model provided by the instrument software (TA Instruments). In the analysis, the stoichiometry of the interaction (n) and the enthalpy change (ΔH) were variable parameters during the fitting. At the same time, the equilibrium dissociation constants (K_i) were fixed at the values obtained in the tryptophan fluorescence quenching competitive binding assay described above. Representative experimental data are shown in **Figure S19**.

Figure S19. Raw data obtained in the ITC experiments. The titration curves (left) and corresponding point diagrams in the coordinates: peptide/protein molar ratio vs. peak area (right)

4-open (Orn-NH-open)

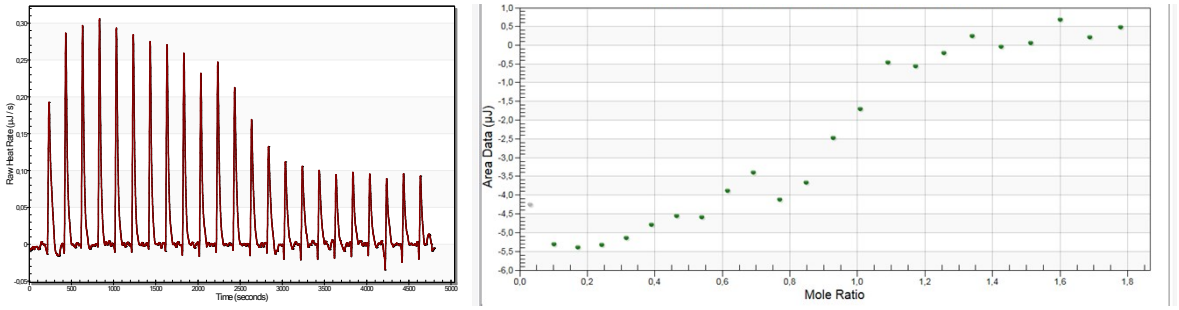

4-closed (Orn-NH-closed)

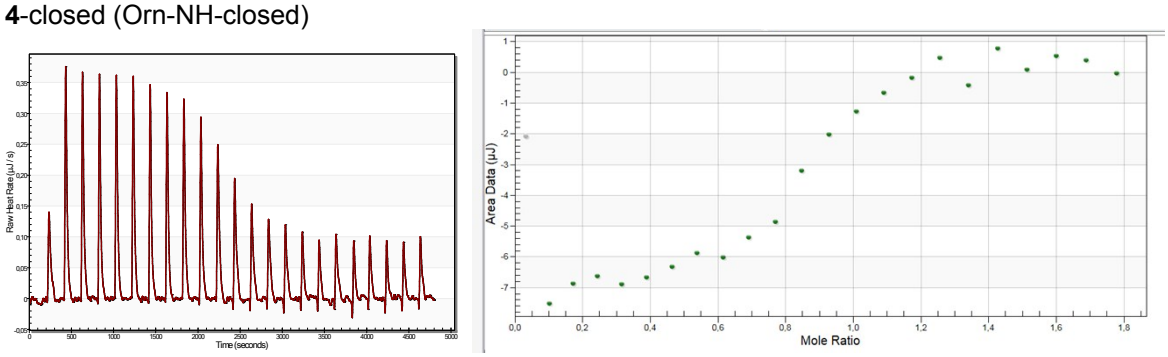

5-open (Orn-NMe-open)

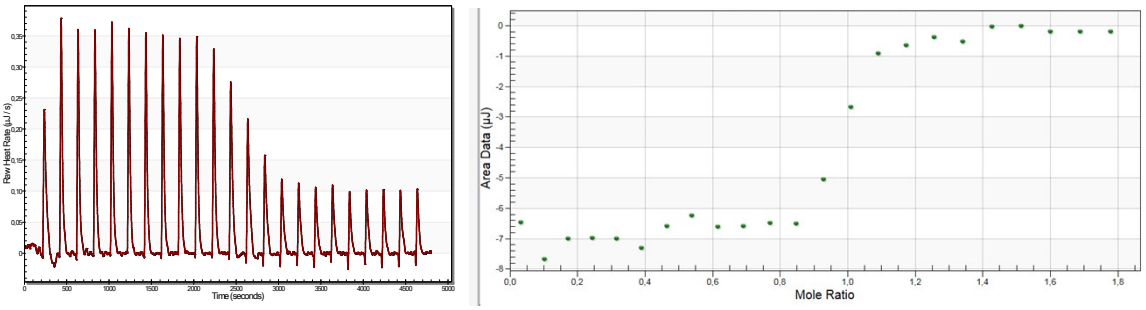

5-closed (Orn-NMe-closed)

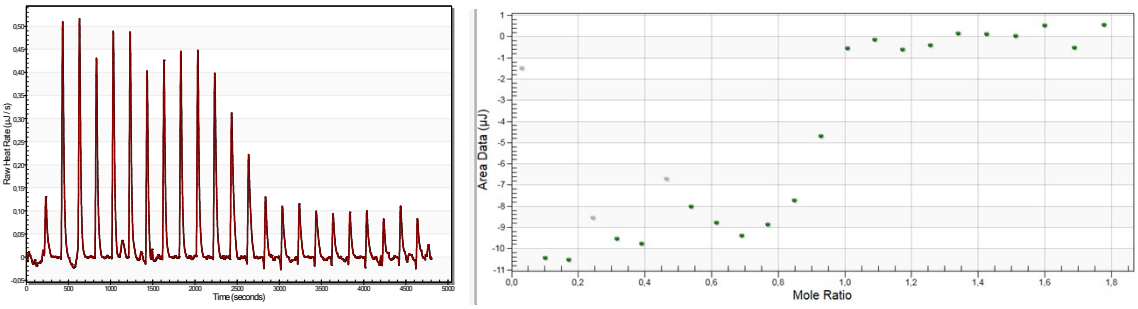

6-open (Lys-NH-open)

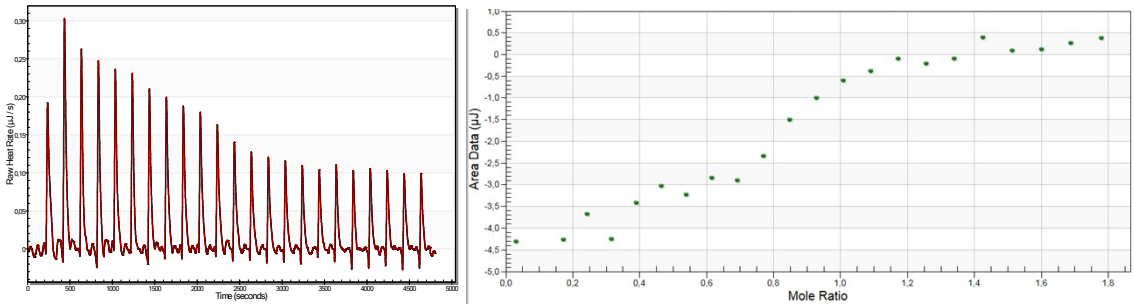

6-closed (Lys-NH-closed)

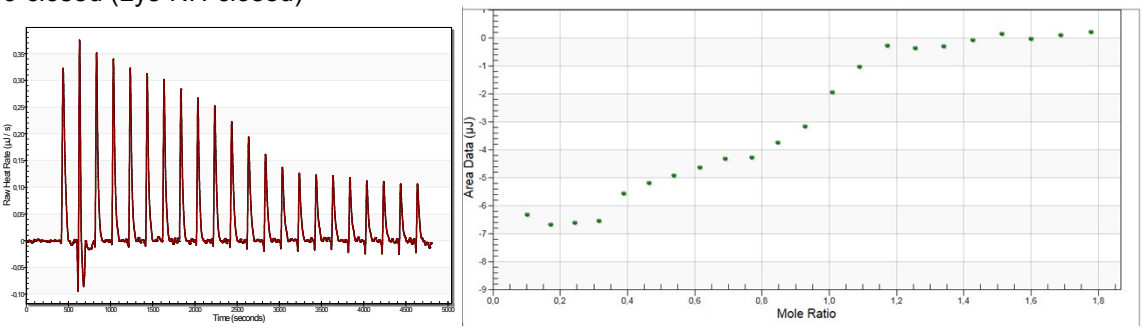

7-open (Lys-NMe-open)

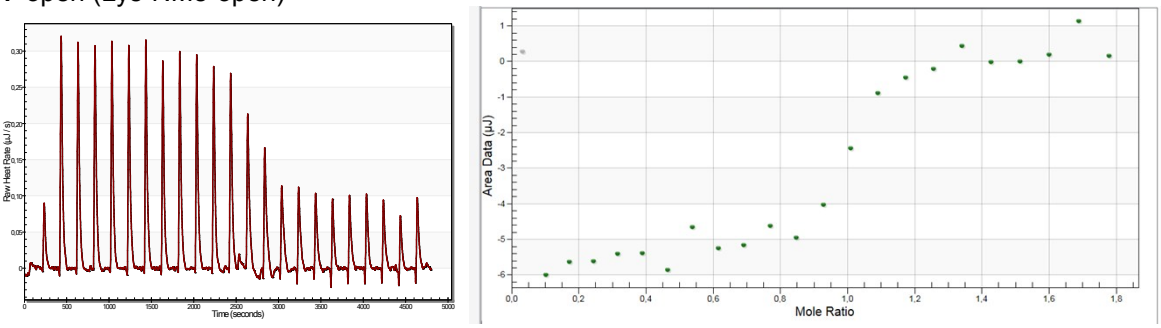

Figure S19. (continued)

7-closed (Lys-NMe-closed)

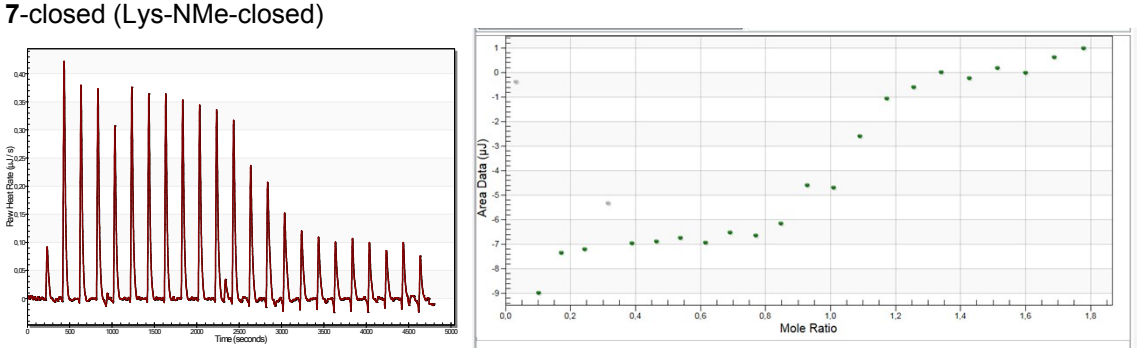

pDI

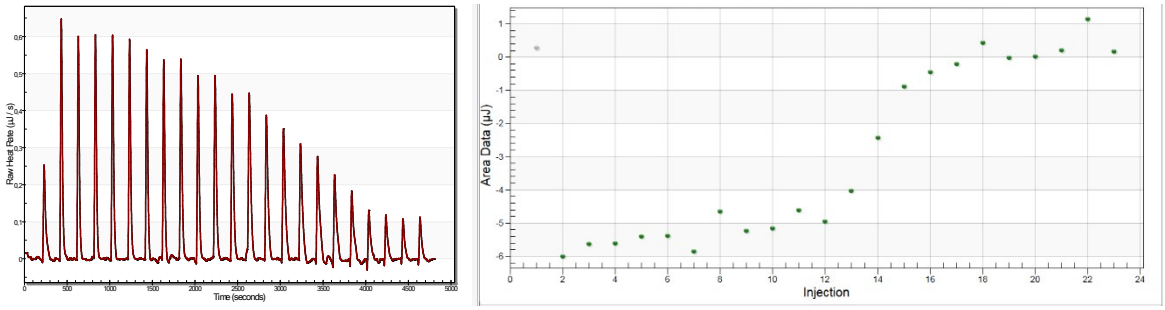

Circular dichroism (CD) spectroscopy

Stock solutions of the peptides (pure "closed" photoforms, 1 mg/mL) were prepared in water-acetonitrile (2:1 vol.) mixtures and aliquots of ca.50 µmol were freeze-dried prior to measurements. The preparations were performed in low light exposure conditions at all stages before *in situ* photoswitching. Appropriate amounts of aqueous buffer (10 mM salt-free phosphate buffer, pH 7.4, supplemented with 0.005% Tween® 20) were added at room temperature to obtain a solution (suspension) at a peptide concentration of ca. 0.1 mg/mL. The solutions (suspensions) were rigorously vortexed/bath-sonified until clear, and immediately transferred to the measurement cuvettes.

Circular dichroism spectra were recorded a Jasco J-815 CD spectropolarimeter using a home-built nitrogen flow regulator. Rectangular quartz cuvettes (Suprasil®) of 1 mm path length from Hellma were used. All spectra were measured at a controlled temperature (25 °C) using the standard Jasco setup of a rectangular sample holder that was connected to an external water thermostat (Julabo). The spectra were recorded from 260 to 185 nm. The measurements were performed in continuous scanning mode using 1 nm spectral bandwidth, 0.1 nm data pitch, and 8 s response time of the detector. Three consecutive scans were collected at a rate of 20 nm/min and averaged for each spectrum, including the backgrounds. After initial measurement, each sample remaining it the cuvette was exposed to irradiation with visible light (LUMATEC Superlite 410 light source, λ_{max} = 550 nm, irradiance ~ 20 mW/cm^2, 10 min) and CD spectra were measured again. The background spectra were subtracted from the sample spectra after the measurements; results were corrected to zero ellipticity at 260 nm, and individually scaled (according to tryptophan absorbance readout after the photoswitching). Spectral acquisition and all processing steps were performed using the preinstalled software package of the spectropolarimeter (Jasco).

Secondary structure analysis was performed using the CDSSTR program with the implemented SVD (singular value decomposition) algorithm [S5]. The analysis algorithm, as well as the protein CD spectra of the reference data set #3, are provided by the DICHROWEB on-line server [S6]. The quality of the fit between experimental and back-calculated spectra corresponding to the derived secondary structure fractions was assessed from the normalized root mean square deviation.

Molecular docking

Molecular docking was performed using a flexible ligand, compound **5** (in the "open" and "closed" photoforms), and a fixed structure of the protein, the p53-interacting domain of the human MDM2 ($MDM2^{6-125}$). We used an algorithm of systematic docking (SDOCK+) implemented in QXP docking software. The maximum number of SDOCK+ routine steps was set to 300, and 10 best structures (based on a built-in QXP scoring function [S7]) were retained for each compound. The pharmacophore model of the protein binding site was derived from our X-ray data (PDB ID: 6Y4Q). Per the defined pharmacophore model, the resulting protein-ligand complex structures were filtered by intrinsic Flo+ filters and multiRMSD [S8]. Filtering was based on such criteria as the built-in QXP scoring function, the number of hydrogen bonds, the protein-ligand contact surface area, and the distance from ligand to crucial points of the corresponding pharmacophore model. The docking results are illustrated in **Figure S20**.

Molecular dynamics simulation (MD)

MD simulation was run to compare and examine the interaction in selected complexes protein/ligand, with "open" and "closed" photoforms of the ligand **5** done separately. The following protocol of MD calculations was applied. All calculations were conducted using the GROMACS 5.1.3 [S9] and the Charmm36 [S10] force field. The complexes were protonated according to the internal GROMACS function "ingh". Topology files for the ligands were generated by Swissparam [S11]. The complexes were solvated with explicit water molecules in TIP3P and placed in the center of a cubic water-filled box. Minimum 0.9 nm distance was maintained between the complex and the edge of the simulation box so that complexes were fully immersed in water and rotated freely. To neutralize/balance the system, Na^+/Cl^- ions were added up to the effective concentration of 0.15 M. To remove "clashes" (i.e., close overlaps of the LJ (Lennard-Jones systems/energy) cores) an energy minimization was performed. For energy minimization, we used the steepest descent minimizer (integrator=steep). Afterward, two-stage equilibrations were done: (1) NVT simulation (with constant Number of particles, Volume, and Temperature) during 100 ps, (2) NPT simulation (with constant Number of particles, Pressure, and Temperature) during one ns. Finally, selected complexes were applied to the MD simulation (100 ns). **Figure S21** illustrates the root mean square deviations (RMSD) for the atoms of the protein and ligands. The Coulomb and Lennard-Jones energies of interactions between $MDM2^{6-125}$ and **5** during the MD simulation time are shown in **Figure S22**.

Figure S20. Docking results. (a) The complex with the "open" photoform of 5; (b) the complex with the "closed" photoform of 5. The ligand is shown in gray/blue/red colors; the protein is drawn in yellow. Amino acid residues of the protein involved in binding are denoted with the three-letter code.

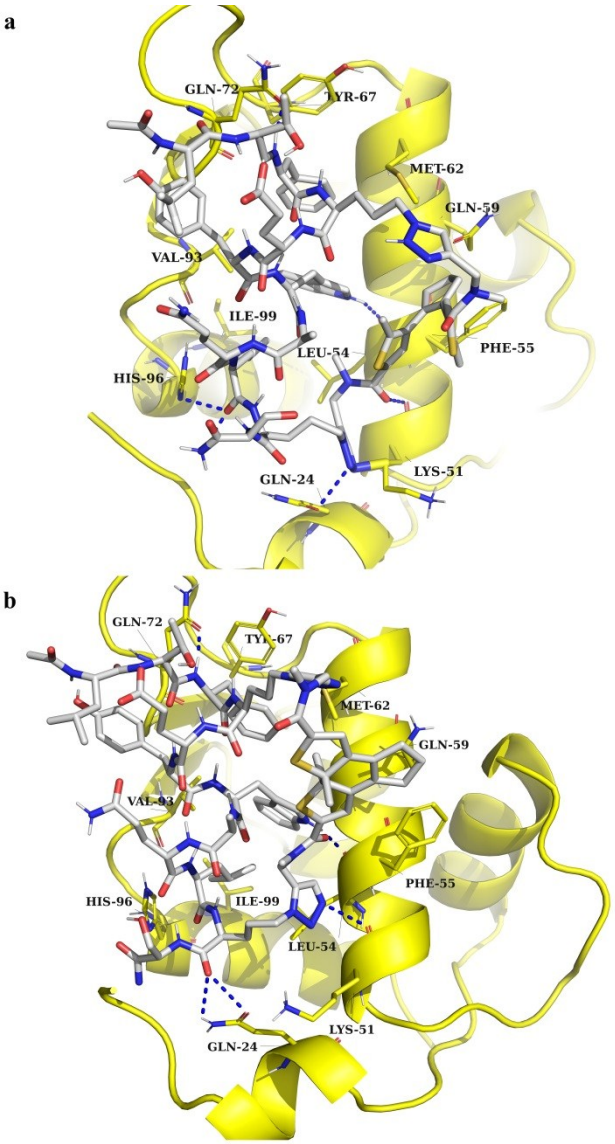

Figure S21. RMSD of (a) free MDM2$^{6-125}$ (green trace), the protein in the complex with 5-"open" (red trace), and 5-"closed" (black trace); (b) the ligand 5 in the 5/MDM2 complexes during the MD simulations. 5-"open" – red trace, 5-"closed" – black trace.

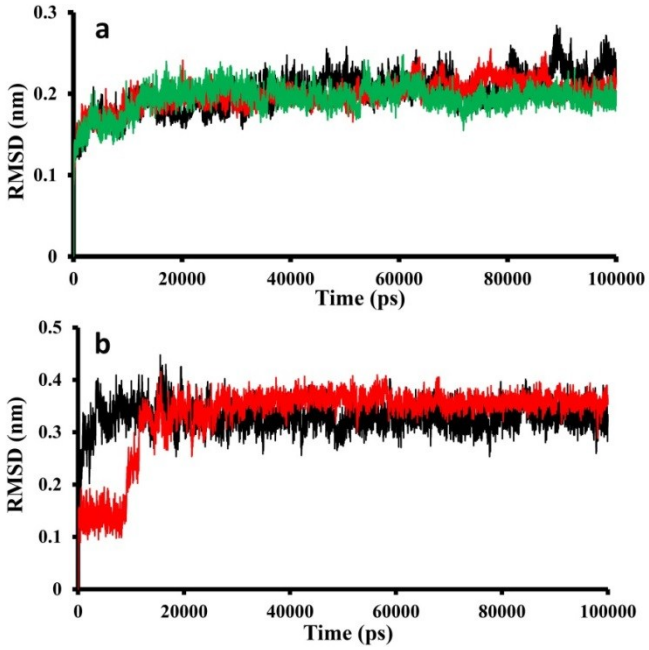

Figure S22. Coulomb (Coul-SR, (a)) and Lennard-Jones (LJ-SR, (b)) energies of interactions between MDM2$^{6-125}$ and 5- "open" (red traces) and 5-"closed" (black traces) photoisomers during the MD simulations.

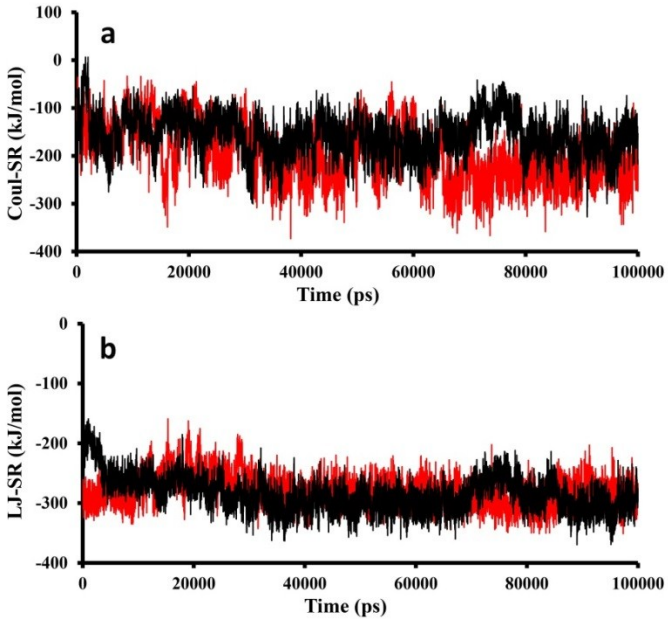

Protein crystallography

Protein-peptide complex purification

The protein-peptide complex was purified, as reported previously [S12].

Crystallization screening

Concentrated complex (~10 mg/mL) was crystal-screened in a 96-well MRC plate format using commercially available screens Wizard I&II and JCSG+ (Molecular Dimensions). The complex was crystallized using the sitting drop vapor diffusion method. Protein was mixed with the crystallization condition in 200:200 nL and 200:100 nL ratios using the Moskito liquid handling robot (TTP Labtech) and incubated at 19 °C. Crystals were obtained under different conditions over 1-3 days.

X-ray diffraction data collection, processing, refinement

Several crystals from different conditions were diffracted at the Diamond Light Source (Harwell, UK) i03 beamline. Majority of crystals diffracted to 1.5-2 Å resolution. Collected native datasets were processed with autoPROC [S13]. Most crystals exhibited identical space group and unit cell parameters. Several datasets having the same crystal form were successfully merged using autoPROC to improve data quality and completeness. Crystallization conditions for the crystals used in the combined datasets are shown in **Table S1**.

Table S1. Crystallization conditions of diffracted MDM2/5-"open" complex crystals

Dataset	Condition
1	10% w/v PEG 8000 (precipitant), 0.1 M Tris-HCl pH 7.0 (buffer), 0.2 M Magnesium chloride hexahydrate (salt)
2	30% v/v PEG 400 (precipitant), 0.1 M CHES-NaOH pH 9.5 (buffer),
3	

The molecular replacement phasing method was applied using the protein structure from PDB ID: 5AFG as a search model. Manual real-space refinement was done in Coot [S14] and automated refinement with phenix.refine [S15] and autoBUSTER [S16].

Linker electron densities were clearly observed before any linker atoms were fitted into the model, as shown in **Figure S23**.

Figure S23. Linker electron densities in the X-ray model of MDM2 in complex with 5-“open”

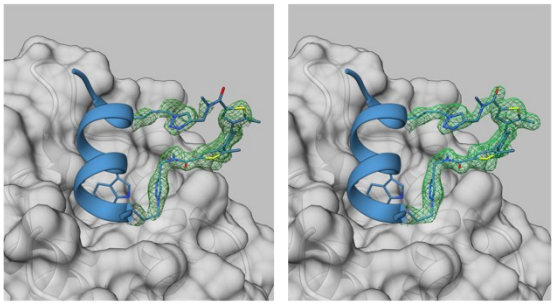

Table S2. Statistics of X-ray crystallographic data collection, processing and refinement

PDB ID:	**6Y4Q**
Ligand	**5**-"open"
Data collection:	
Collection date	20181021
Synchrotron	Diamond Light Source
Beamline:	I03
X-ray wavelength:	0.9762Å
Data processing*:	
Spacegroup	P 1
Unit cell (a, b, c [Å],	34.240 34.840 48.410
α,β,γ [°])	93.38 107.38 117.45
Resolution limits [Å]	44.93-1.63 (1.72-1.63)
Number of molecules in ASU	2
No of total/unique reflections	65928/21777
Multiplicity	3.0 (1.7)
Rmerge	0.162 (0.462)
Rmeas	0.184 (0.654)
I/σI	23.3 (4.4)
CC1/2	0.987 (0.712)
Completeness [%]	94.9 (88.6)
Refinement:	
Rwork/Rfree [%]	0.194/0.229
Number of unique/free reflections used	21751/1086
R.m.s deviations:	
bond lengths [Å]	0.014
bond angles [°]	1.581
Ramachandran analysis:	
Most favoured	198 (99.0%)
Allowed	2 (1.0%)
Outliers	0 (0.0%)
Mean/Wilson B-factor	30.76/ 24.98

(*Values for the high-resolution shell are given in parenthesis)

References

[S1] O. Babii, S. Afonin, M. Berditsch, S. Reiβer, P.K. Mykhailiuk, V.S. Kubyshkin, T. Steinbrecher, A.S. Ulrich, I.V. Komarov, *Angew. Chem. Int. Ed.* **2014**, *53*, 3392.

[S2] Y. Lau, Y. Wu, P. de Andrade, W.R.J.D. Galloway, D.R. Spring*, Nat. Protoc.* **2015**, *10***,** 585.

[S3] D. Beckett. *Methods in Enzymology*, **2011**, *488*, 1.

[S4] C.J. Brown, S.T. Quah, J. Jong, A.M. Goh, P.C. Chiam, K.H. Khoo, M.L. Choong, M.A. Lee, L. Yurlova, K. Zolghadr, T.L. Joseph, C.S. Verma, D.P. Lane, *ACS Chem. Biol*. **2012**, *8*, 506.

[S5] N. Sreerama and R.W. Woody, *Anal. Biochem.* **2000**, *287*, 252, and references cited therein

[S6] L. Whitmore and B.A. Wallace, *Nucleic Acids Res*. **2004**, *32*, W668

[S7] C. McMartin and R.S. Bohacek, *J. Comput. Aided Mol. Des*. **1997**, *11*, 333.

[S8] O.O. Sudakov, O.M. Balinskyi, M.O. Platonov, D.B. Kovalskyy, *Biopolym. Cell*. **2013**, *29*, 418.

[S9] D. Van der Spoel, E. Lindahl, B. Hess, The GROMACS development team GROMACS User Manual version 4.6.5. 2013.

[S10] J. Huang and A.D. MacKerell Jr., *J. Comput. Chem.* **2013**, *34*, 2135.

[S11] V. Zoete, M. A. Cuendet, A. Grosdidier, O. Michielin, *J. Comput. Chem*. **2011**, *32*, 235.

[S12] Y. H. Lau, Y. Wu, M. Rossmann, B. X. Tan, P. de Andrade, Y. S. Tan, C. Verma, G. J. McKenzie, A. R. Venkitaraman, M. Hyvönen, D. R. Spring, *Angew. Chem. Int. Ed.* **2015**, *54*, 15410.

[S13] C. Vonrhein, C. Flensburg, P. Keller, A. Sharff, O. Smart, W. Paciorek, T. Womack, G. Bricogne. *Acta Cryst.* **2011**, *D67*, 293.

[S14] P. Emsley, B. Lohkamp, W.G. Scott, K. Cowtan. *Acta Cryst.* **2010**, *D66*, 486.

[S15] P.V. Afonine, R. W. Grosse-Kunstleve, N. Echols, J. J. Headd, N. W. Moriarty, M. Mustyakimov, T. C. Terwilliger, A. Urzhumtsev, P. H. Zwart, P. D. Adams. *Acta Cryst.*, **2012**, *D68*, 352.

[S16] Bricogne, G. *et al.* (**2017**) 'BUSTER version 2.10.3.' Global Phasing Ltd., Cambridge, United Kingdom.